The extent of pollution and bioaccessibility of lead and zinc from a legacy mine in Kabwe, Zambia, and immobilization of toxic elements by half-burnt dolomite

A dissertation submitted in partial fulfillment of the requirements for the degree of Doctorate in Engineering

By

MUFALO WALUBITA

Division of Sustainable Resources Engineering
Graduate School of Engineering,
Hokkaido University, Japan.

2022

ABSTRACT

Kabwe is a town in the central province of Zambia that has been a global site of concern due to the historic mining of lead (Pb) and zinc (Zn). The production of the mineral resources ceased after the depletion of the ore body in 1994. The by-products from the mining activities were left unattended; consequently, pollution of the surrounding environment was inevitable. The by-products from the legacy mine include slag heaps, mining residue materials (MRM), and waste rocks. These mine wastes contain potentially toxic elements (PTEs) such as Pb and Zn. The children are particularly the most vulnerable to Pb intoxication. This is because they frequently explore their environment through hand-to-mouth activities, subsequently may increase their Pb uptake from the polluted environment through accidental ingestion or inhalation. Thus, it is imperative to understand the sources of Pb intoxication, the extent of pollution, bioaccessibility of PTEs, and possible remediation technology to reduce the contamination levels of PTEs from the historic mine. Of all the mine wastes in Kabwe, the MRM occupies a more extensive area, and surrounding soils such as playground soils (SPs) are a potential source of Pb intoxication for the children of Kabwe. Therefore, this study focussed on the MRM and the SPs near a legacy mine in Kabwe, Zambia. The leaching behavior, the extent of pollution in SPs, solid-phase partitioning, and bioaccessible fractions of Pb and Zn in various particle sizes, coupled with the solubility of the elements from MRM and SPs in simulated fluids, were analyzed. The study is significant for bridging the gap between previously reported high blood Pb levels and the bioaccessible Pb and Zn in the MRM and the SPs. Finally, and countermeasures against reducing Pb and Zn in MRM by half-burnt dolomite (HBD) were also investigated. The dissertation contains five chapters.

In chapter 1, the general introduction of Pb contamination in Kabwe is briefly reviewed and introduced. The necessities and objectives of the present study are then depicted.

In chapter 2, the extent of pollution and leaching behavior of the elements from SPs were investigated. Kabwe mine wastes are responsible for contaminating the surrounding soil and dust in the Kabwe district. Unfortunately, these wastes arise from the historical mining activities of Pb and Zn, which lacked adequate waste management strategies. As a result, the contaminants like Pb and Zn have spread across the Kabwe

district. To assess the soil pollution derived from the previous mining activities, we characterized topsoil samples (n = 8) from the SPs. In this study, the degree of contamination, geochemical partitioning, and leachability, coupled with the release and retention of Pb and Zn, were studied. The SPs were classified as extremely enriched (enrichment factor > 40) and contaminated with Pb (geo-accumulation index > 5). On average, Pb (up to 89%) and Zn (up to 69%) were bound with exchangeable, weak acid-soluble, reducible and oxidizable phases, which are considered 'geochemically mobile' phases in the environment. The leachates from the soils (n = 5) exceeded the Zambian standard for Pb in potable drinking water (Pb < 0.01 mg/L). Furthermore, the spatial distribution of Pb and Zn showed a significant reduction in contents of Pb and Zn with the distance from the mine area.

In chapter 3, sequential extraction of Pb and Zn in MRM with different particle sizes and their solubility in simulated fluids were investigated. Based on the previous studies showing that some of the residents of Kabwe had high blood Pb levels above recommended value, simulated fluids representing lung conditions (artificial lysosomal fluid (ALF), gamble solution (GS), and phosphate-buffered saline (PBS) were used to assess the solubility of Pb and Zn in the dust (< 30 μm) of MRM samples. Both Pb and Zn were soluble with ALF. However, only Zn was detected with GS and PBS. About 2.9% of Pb was bioaccessible with ALF in MRM and up to 37% of Pb was bioaccessible in the SPs samples. Compared with solubility by oral intake using HC*l*, higher bioaccessible fractions of Pb and Zn were recorded in both MRM and SPs. Different particle size distributions of MRM did not significantly affect the solid-phase partitioning of Pb and Zn in the residues. However, in case of accidental ingestion, substantial amounts of Pb and Zn from the exchangeable phase, carbonates, and Fe/Mn oxides could be available for adsorption in the bloodstream from the MRM and SPs samples. The results suggest that oral intake of contaminated wastes could be considered a more significant route for Pb uptake than inhalation. These findings may explain the high blood Pb levels previously reported in Kabwe.

In chapter 4, the countermeasures for reducing Pb and Zn in MRM were elucidated by using HBD in column and pilot-scale experiments. In this study, the efficacy of the HBD was evaluated by mixing MRM with 1, 5, and 10% ratios of the HBD in columns. The leaching of Pb and Zn was compared with the addition of 10% HBD to

MRM in pilot-scale experiments. Measurements of mineralogical and chemical constituents of the MRM, sequential extraction, and thermodynamic modeling of the leachates using Phreeqc code were carried out to determine the attenuation mechanisms of Pb and Zn. The sources of Pb and Zn in the MRM were mainly from the exchangeable and carbonate fractions. The SEM-EDS observations suggest that Pb and Zn were primarily associated with sulfide minerals although XRD did not detect the sulfide minerals in MRM. The dissolution of secondary soluble sulfate minerals contributed to leaching of Pb and Zn. The introduction of HBD into the MRM increased effluent pH and decreased the leaching concentrations of Pb and Zn. The addition of 10% HBD was enough to suppress the leaching of Pb and Zn in both the column and pilot-scale experiments. The saturation indices suggest that the retention mechanisms of Pb and Zn by HBD accredit to precipitation, co-precipitation, and adsorption reactions. These results present an effective, inexpensive, and long-term immobilization technology for toxic elements in hazardous wastes from legacy mines.

Chapter 5 summarizes all general conclusions of the present study. The results could provide the fundamental knowledge of the leachability, geochemical partitioning and bioaccessibility of Pb and Zn in Kabwe, Zambia. Chemical immobilization by HBD could be a possible remediation technology for the legacy mine.

TABLE OF CONTENTS

LIST OF FIGURES

LIST OF TABLES

Chapter 1

GENERAL INTRODUCTION

1.1 Background

Lead (Pb) is one of the toxic elements naturally found in the earth's crust. From time in memorial, Pb has been mined and processed from different parts of the world because of its essential uses in paints, solder, jewelry, toys, cosmetics, and traditional medicines (WHO, 2017). The profound use has resulted in extensive environmental pollution, human exposure, and significant public health problems in many parts of the world (Fuller et al., 2022). Due to its toxic effects, once ingested via contaminated soil, food, or inhalation from the atmosphere, the Pb adsorbed in the bloodstream tends to form covalent bonds with organic groups and generate toxic effects when they bind to cellular macromolecules (Bian et al., 2015, Cao et al., 2016, Nag and Cummins, 2022). Serious health consequences may arise from these toxicological changes (Briffa et al., 2020). High levels of Pb intoxication may affect the brain and the central nervous system, resulting in impaired functioning (WHO, 2017). The children are the most affected by Pb intoxication because it attacks their brain development, resulting in a reduced intelligence quotient, leading to poor school performance and lower tertiary education attainment (Elbaz-Poulichet et al., 2017, Heidari et al., 2022, Yabe et al., 2020). Although Pb mining has substantial economic benefits, the effects of Pb pollution from legacy mines have been reported worldwide (Hansson et al., 2019, Helser and Cappuyns, 2021; Reyes et al., 2021). One legacy mine of global concern is the historical Pb mining in Zambia's Kabwe town which left a legacy of environmental pollution and childhood Pb poisoning.

1.2 Historic Pb mining

Over the past years, pollution of Pb and Zinc (Zn) has been reported in Kabwe, Zambia because of historic mining of Pb-Zn (Tembo et al., 2006). The exploitation of the mineral resources commenced in 1904 (Southwood et al., 2019). With a lifespan of at least 90 years of underground mining and smelting, the mine produced 0.8 Mt of Pb and 1.8 Mt of Zn, as well as minor amounts of Ag (79 t), V_2O_5 (7820 t), Cd (235 t) and Cu (64 t) as by-products (Kamona and Friedrich, 2007). Mining of the Pb-Zn brought economic development to the city of Kabwe, however, massive amounts of mine wastes

were left unattended after the mine closure in 1994. In addition, no pollution law regulated the discharge of mine wastes up until 1990 (EPPCA, 1990).

1.3 Pollution in Kabwe

The by-products of the legacy mine in Kabwe include slags heaps, residue materials, tailings, and mixed wastes, which remain in huge amounts (Tangviroon et al., 2020, Silwamba et al., 2020). Therefore, the distribution and transportation of toxic elements from the mine wastes to the surrounding environment are inevitable. Nakamura et al. (2021) highlighted that the dispersion of aerosols from the dumping site was responsible for the contamination in the surrounding soils due to wind direction, the distance from the mine site, humidity, and particle size of aerosols, which greatly affected the dispersion of dust/mine wastes containing Pb. For example, the total content of Pb in soils collected from playground soils decreased with distance from the dumping area, and the amount deposited at each playground soils (Mufalo et al., 2021) was affected by winds from various directions. Baieta et al. (2021) also assessed soil profiles around the smelter in Kabwe and two pine trees for tree ring cores. High contents of metals were present only in the top layers of soil and were higher in soils closer to the smelter (up to 16,000 mg/kg Pb; 14,000 mg/kg Zn) compared to remote soils (up to 194 mg/kg Pb; 438 mg/kg Zn). The heavy metals were also present in trees further away from the dumping site with concentrations up to 6.48 mg/kg Pb: 10.6 mg/kg Zn, possibly due to the deposition of wind-blown particles. The findings from Baieta et al. (2021) were in good agreement with the simulations by Nakamura et al. (2021). In addition, spatial mapping of Pb and Zn in Kabwe town showed that the heavy metals were more concentrated around the mine area and gradually reduced with distance further away from the source (Figure 1) and that the Pb and Zn contents in topsoils were found to be significantly higher compared to the permissible ecological limits used in Canada for soil quality guidelines in residential areas (Pb 140 mg/kg, Zn 200 mg/kg) (Kříbek et al., 2019)

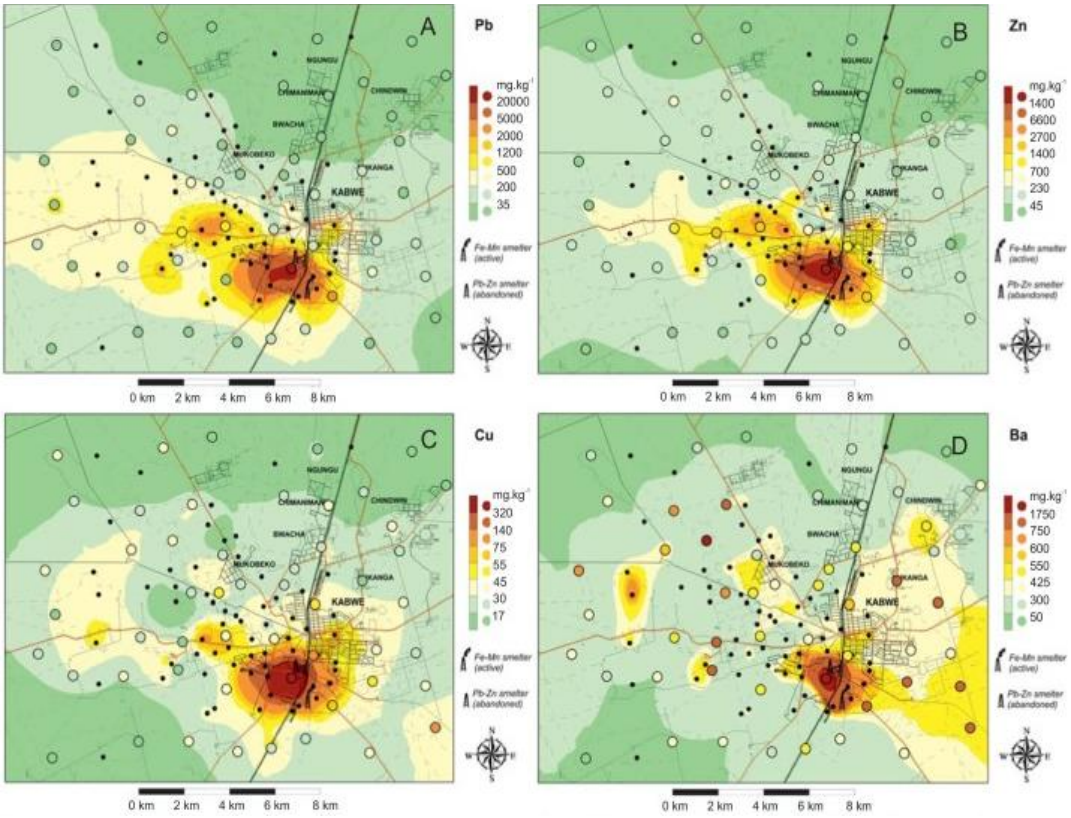

Figure 1. Contour maps of the Pb (A), Zn (B), Cu (C) and Ba (D), contents (in mg/kg) in topsoil (0-3 cm depth) and classed point maps of the same elements in subsurface soils (70-80 cm depth) in the Kabwe area, Zambia (Kříbek et al., 2019).

1.4 The extent of Pb intoxication

The high contents of toxic elements in the soils negatively impacted the residents of Kabwe, especially the children. Due to children's hand-to-mouth activities, they ingest toxic elements in high quantities. Bose-O'Reilly et al. (2018) pointed out that 95% of children living in some townships of Kabwe had elevated blood lead levels (BLLs) > 10 µg/dL, and approximately 50% of those children recorded BLLs ≥ 45 µg/dL. These findings revealed extensive Pb poisoning in children and therapy was recommended, especially for those exceeding ≥ 45 µg/dL. A study by Toyomaki et al. (2021) also revealed high Pb contents in infants' feces with mean values of (39.2 mg/kg) and maximum content of 3,002 mg/kg. Moreover, the spatial hotspots for Pb intoxication (BLLs) were concentrated in townships near the mine area with a confidence level of 99% (Figure 2) (Moonga et al., 2021).

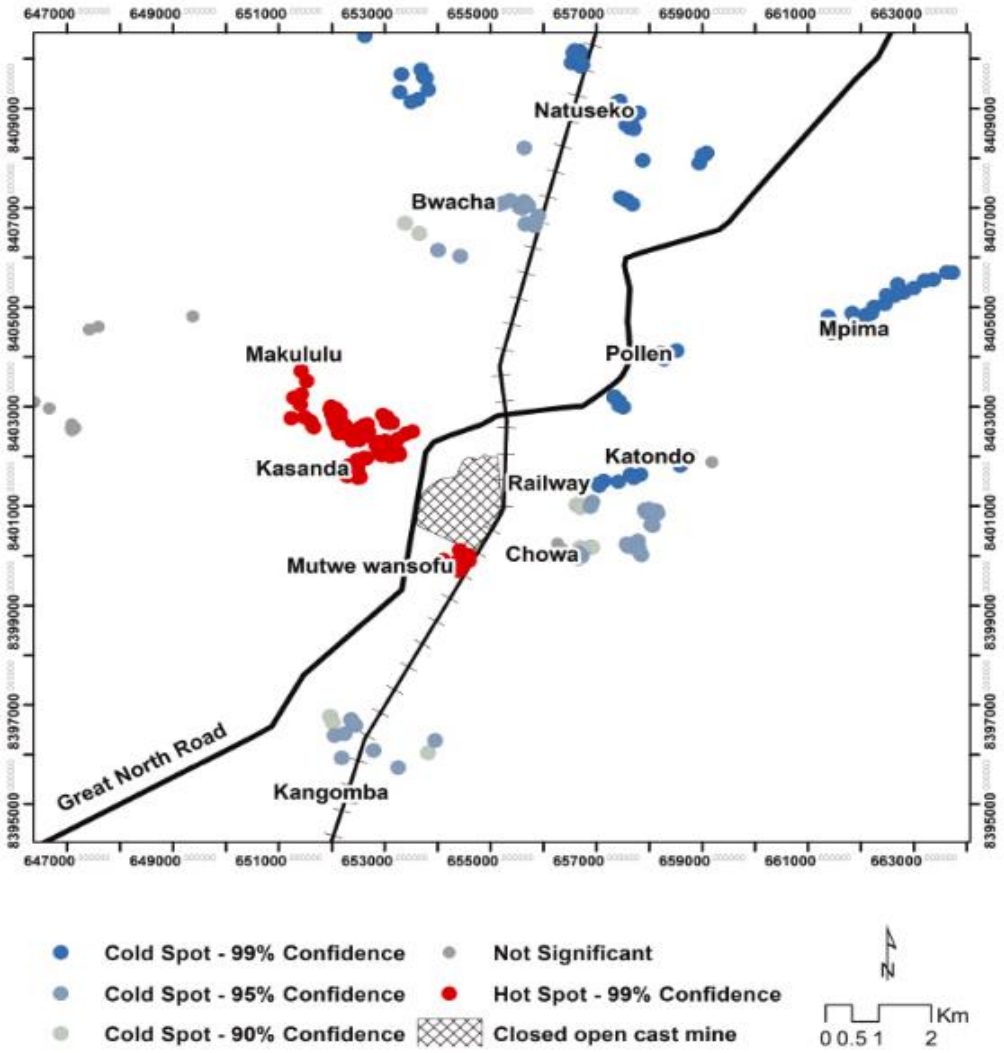

Figure 2. Spatial distribution of blood lead levels among the children in Kabwe, Zambia (Moonga et al., 2021)

1.5 Remediation proposals

A few studies have been conducted on the remediation of the legacy mine in Kabwe. For example, Kříbek et al. (2019) performed laboratory tests using humate or phosphate solution to reduce the dissolution of Pb when digested with glycine. However, the gastric bioaccessible fractions in treated and untreated soil samples were the same. Therefore, only plant-available metals decreased when treated with phosphate or humate-phosphate mixtures. Mwandira et al. (2019) also stressed the use of bacteria to remediate the dumping site via capping mine wastes of Kabwe using microbially induced calcium carbonate precipitation (MICP). The results revealed that the bacteria reduced the entrance of water and oxygen into the dump, consequently reducing the leaching of heavy

metals. However, such proposals could be costly to implement on a larger scale. For example, the mining residue materials (MRM) occupy a large area around the dump site and could be impossible to remediate using the highlighted technique effectively. The author's previous studies investigated several potential chemical immobilizers (magnesium oxide, raw dolomite, and half-burnt dolomite) to remediate Pb and Zn leached from the MRM (Tangviroon et al., 2020). Among all selected immobilizers, half-burnt dolomite (HBD) has proven to be the most promising immobilizer since it could effectively immobilize both Pb and Zn. However, the analyses were done based on the batch leaching, where the HBD was added to the MRM in a predetermined volume of water and then shaken for a set period, thus allowing us to assess the immobilization potential of the HBD. In other words, the batch leaching experiments did not seem to be a practical prediction of the actual transport of contaminants due to several reasons, such as different solid-to-liquid ratios and flow paths of water from those in the field. (Tabelin et al., 2014).

1.6 Problem statement

The high BLLs in the children previously recorded highlights the severe Pb intoxication problem in Kabwe residents; thus, understanding the factors affecting the release of Pb and Zn in the potential sites for Pb intoxication, such as playground soils (SPs), helps us understand the factors leading to Pb and Zn bioaccessibility in such environments. On the other hand, the MRM significantly contributes to the pollution problem of the surrounding soils. Thus, remediation of the source (MRM) using actual flow conditions in column and pilot-scale experiments could help us understand the attenuation mechanisms of Pb and Zn in the actual environment.

1.7 Purpose of study

Therefore, the purposes of this study were to:

1. Investigate the extent of pollution in SPs near the mine site and understand the factors affecting the solid partitioning, release, and retention of Pb and Zn in the SPs.
2. Evaluate the solid-phase partitioning of Pb and Zn in different particle size of MRM.

3. Find the solubility and bioaccessible fractions of Pb and Zn in MRM and SPs using simulated fluids (artificial lysosomal fluid (ALF), gamble solution (GS), phosphate-buffered saline (PBS) and hydrochloric acid (HC*l*).
4. To find the efficacy of HBD in reducing the Pb and Zn in MRM via assessments in column and validation in pilot-scale experiments.

1.8 Study site

The MRM was randomly collected from dumping site in Kabwe, while the soil samples (SPs) were collected within a 10 km radius in the west and northwest of the mine area (Figure 3). The prevailing winds are usually downwind of the mine site, to the west-northwest direction (Kříbek et al., 2019). Using a stainless-steel hand shovel, soil samples were collected from topsoil (about 5 cm deep) with 3 to 4 mixing points for each sample. A total of 8 soil samples were collected from a community ground in Kasanda area (S1), Makululu primary school (S2), Malumbo community ground (S3), Makululu day secondary (S4), Makululu day secondary garden (S5), David Ramushu secondary school (S6), David Ramushu secondary school garden (S7), and Kebar Christian academy (S8). These samples were stored in airtight vacuum bags and then shipped to Hokkaido University, Japan. The soil samples and MRM were then dried at room temperature before characterization, sequential extraction, and leaching experiments.

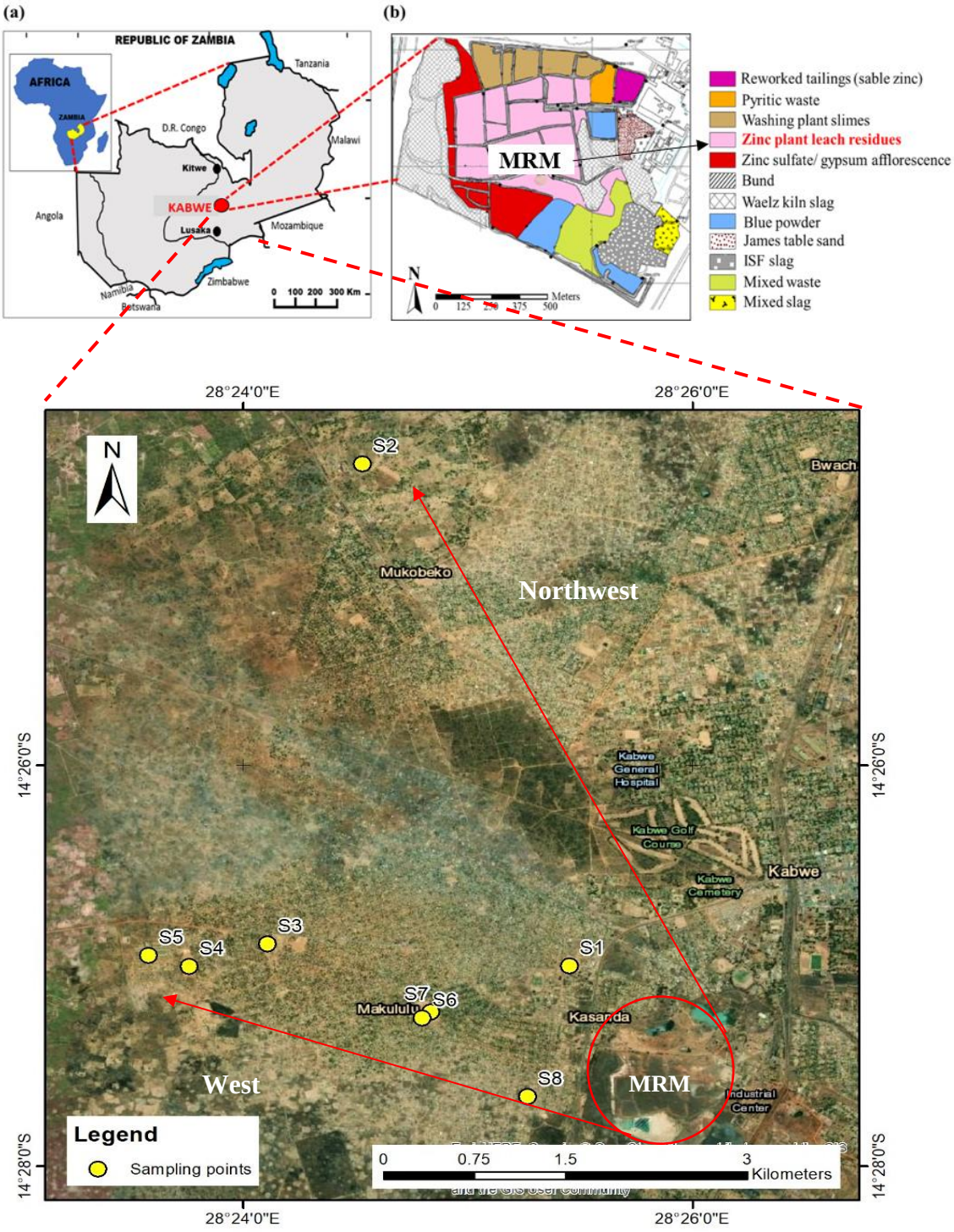

Figure 3. Map of Zambia, showing location of Kabwe (a), location of mining residual materials (MRM) (b) and sampling points for playground soils (SPs) S1, S2, S3, S4, S5, S6, S7 and S8. Image modified from (Mufalo et al., 2021, Silwamba et al., 2020)

1.9 Outline of dissertation

The dissertation consists of five chapters. The content of each chapter is shown below:

In chapter 1, general introduction including the background, problem statement and contents of this study is described.

In chapter 2, the extent of pollution and leaching behavior of Pb and Zn from SPs were investigated, including the solid-phase partitioning of the soils and the influence of the distance from mine area on the contents of Pb and Zn in the playground soils.

In chapter 3, the bioaccessibility of Pb and Zn in the dust (< 30 μm) of the MRM and SPs were investigated. Solubility assessments of Pb and Zn were performed using simulated; artificial lysosomal fluid (ALF), gamble solution (GS), and phosphate-buffered saline (PBS) and compared with hydrochloric acid (HC*l*). The influence of particle size variability in the solid-phase partitioning of MRM was also evaluated.

In Chapter 4, the efficacy of HBD was assessed in column experiments and compared to the pilot experiments in the field. The immobilization was assessed through the leaching of hazardous heavy metals (Pb and Zn).

In chapter 5, general conclusion based on the results obtained in this study was summarized.

.

References

Baieta, R., Mihaljevič, M., Ettler, V., Vaněk, A., Penížek, V., Trubač, J., Kříbek, B., Ježek, J., Svoboda, M., Sracek, O. and Nyambe, I., 2021. Depicting the historical pollution in a Pb–Zn mining/smelting site in Kabwe (Zambia) using tree rings. Journal of African Earth Sciences, 181, 104246.

Bian, B., Zhou, L.J., Li, L., Lv, L. and Fan, Y.M., 2015. Risk assessment of heavy metals in air, water, vegetables, grains, and related soils irrigated with biogas slurry in Taihu Basin, China. Environmental Science and Pollution Research, 22(10), pp. 7794-7807.

Bose-O'Reilly, S., Yabe, J., Makumba, J., Schutzmeier, P., Ericson, B. and Caravanos, J., 2018. Lead intoxicated children in Kabwe, Zambia. Environmental Research, 165, pp. 420-424.

Briffa, J., Sinagra, E. and Blundell, R., 2020. Heavy metal pollution in the environment and their toxicological effects on humans. Heliyon, 6(9), 04691.

Cao, S., Duan, X., Zhao, X., Chen, Y., Wang, B., Sun, C., Zheng, B. and Wei, F., 2016. Health risks of children's cumulative and aggregative exposure to metals and metalloids in a typical urban environment in China. Chemosphere, 147, pp. 404-411.

Elbaz-Poulichet, F., Resongles, E., Bancon-Montigny, C., Delpoux, S., Freydier, R. and Casiot, C., 2017. The environmental legacy of historic Pb-Zn-Ag-Au mining in river basins of the southern edge of the Massif Central (France). Environmental Science and Pollution Research, 24(25), pp. 20725-20735.

EPPCA-Environmental Protection and Pollution Control Act (1990). Environmental Council of Zambia (ECZ), Act No. 12

Fuller, R., Landrigan, P.J., Balakrishnan, K., Bathan, G., Bose-O'Reilly, S., Brauer, M., Caravanos, J., Chiles, T., Cohen, A., Corra, L. and Cropper, M., 2022. Pollution and health: a progress update. The Lancet Planetary Health.

Hansson, S.V., Grusson, Y., Chimienti, M., Claustres, A., Jean, S. and Le Roux, G., 2019. Legacy Pb pollution in the contemporary environment and its potential bioavailability in three mountain catchments. Science of the Total Environment, 671, pp. 1227-1236.

Heidari, S., Mostafaei, S., Razazian, N., Rajati, M., Saeedi, A. and Rajati, F., 2022. The effect of lead exposure on IQ test scores in children under 12 years: a systematic review and meta-analysis of case-control studies. Systematic Reviews, 11(1), pp. 1-8.

Helser, J. and Cappuyns, V., 2021. Trace elements leaching from pbzn mine waste (plombières, belgium) and environmental implications. Journal of Geochemical Exploration, 220, 06659.

Kamona, A.F. and Friedrich, G.H., 2007. Geology, mineralogy and stable isotope geochemistry of the Kabwe carbonate-hosted Pb–Zn deposit, Central Zambia. Ore Geology Reviews, 30(3-4), pp. 217-243.

Kříbek, B., Nyambe, I., Majer, V., Knésl, I., Mihaljevič, M., Ettler, V., Vaněk, A., Penížek, V. and Sracek, O., 2019. Soil contamination near the Kabwe Pb-Zn smelter in Zambia: Environmental impacts and remediation measures proposal. Journal of Geochemical Exploration, 197, pp. 159-173.

Moonga, G., Chisola, M.N., Berger, U., Nowak, D., Yabe, J., Nakata, H., Nakayama, S., Ishizuka, M. and Bose-O'Reilly, S., 2022. Geospatial approach to investigate spatial clustering and hotspots of blood lead levels in children within Kabwe, Zambia. Environmental Research, 207, 112646.

Mufalo, W., Tangviroon, P., Igarashi, T., Ito, M., Sato, T., Chirwa, M., Nyambe, I., Nakata, H., Nakayama, S. and Ishizuka, M., 2021. Solid-Phase partitioning and leaching behavior of Pb and Zn from playground soils in Kabwe, Zambia. Toxics, 9(10), 248.

Mwandira, W., Nakashima, K., Kawasaki, S., Ito, M., Sato, T., Igarashi, T., Chirwa, M., Banda, K., Nyambe, I., Nakayama, S. Nakata, H. and Ishizuka M., 2019.

Solidification of sand by Pb (II)-tolerant bacteria for capping mine waste to control metallic dust: Case of the abandoned Kabwe Mine, Zambia. Chemosphere, 228, pp. 17-25.

Nag, R. and Cummins, E., 2022. Human health risk assessment of lead (Pb) through the environmental-food pathway. Science of the Total Environment, 810, 151168.

Nakamura, S., Igarashi, T., Uchida, Y., Ito, M., Hirose, K., Sato, T., Mufalo, W., Chirwa, M., Nyambe, I., Nakata, H., Nakayama, S. and Ishizuka M., 2021. Evaluation of dispersion of Lead-Bearing Mine Wastes in Kabwe District, Zambia. Minerals, 11(8), 901.

Reyes, A., Cuevas, J., Fuentes, B., Fernandez, E., Arce, W., Guerrero, M. and Letelier, M.V., 2021. Distribution of potentially toxic elements in soils surrounding abandoned mining waste located in Taltal, Northern Chile. Journal of Geochemical Exploration, 220, 106653.

Silwamba, M., Ito, M., Hiroyoshi, N., Tabelin, C.B., Fukushima, T., Park, I., Jeon, S., Igarashi, T., Sato, T., Nyambe, I, Chirwa, M., Nakata H, Nakayama S. and Ishizuka M., 2020. Detoxification of lead-bearing zinc plant leach residues from Kabwe, Zambia by coupled extraction-cementation method. Journal of Environmental Chemical Engineering, 8(4), 104197.

Southwood, M., Cairncross, B. and Rumsey, M.S., 2019. Minerals of the Kabwe ("Broken Hill") mine, central province, Zambia. Rocks & Minerals, 94(2), pp. 114-149.

Tabelin, C.B., Hashimoto, A., Igarashi, T. and Yoneda, T., 2014. Leaching of boron, arsenic and selenium from sedimentary rocks: II. pH dependence, speciation and mechanisms of release. Science of the Total Environment, 473, pp. 244-253.

Tangviroon, P., Noto, K., Igarashi, T., Kawashima, T., Ito, M., Sato, T., Mufalo, W., Chirwa, M., Nyambe, I., Nakata, H, Nakayama, S and Ishizuka, M., 2020. Immobilization of lead and zinc leached from mining residual materials in Kabwe, Zambia: Possibility of chemical immobilization by dolomite, calcined dolomite, and magnesium oxide. Minerals, 10(9), 763.

Tembo, B.D., Sichilongo, K. and Cernak, J., 2006. Distribution of copper, lead, cadmium and zinc concentrations in soils around Kabwe town in Zambia. Chemosphere, 63(3), pp. 497-501.

Toyomaki, H., Yabe, J., Nakayama, S.M., Yohannes, Y.B., Muzandu, K., Mufune, T., Nakata, H., Ikenaka, Y., Kuritani, T., Nakagawa, M, Choongo, K and Ishizuka., 2021. Lead concentrations and isotope ratios in blood, breastmilk and feces: Contribution of both lactation and soil/dust exposure to infants in a lead mining area, Kabwe, Zambia. Environmental Pollution, 286, 117456.

Yabe, J., Nakayama, S.M., Nakata, H., Toyomaki, H., Yohannes, Y.B., Muzandu, K., Kataba, A., Zyambo, G., Hiwatari, M., Narita, D. and Yamada, D., 2020. Current trends of blood lead levels, distribution patterns and exposure variations among household members in Kabwe, Zambia. Chemosphere, 243,125412.

World Health Organization, 2017. Lead poisoning and health fact sheet.

Chapter 2

SOLID-PHASE PARTITIONING AND LEACHING BEHAVIOR OF LEAD AND ZINC FROM PLAYGROUND SOILS IN KABWE, ZAMBIA

2.1 Introduction

Kabwe town is considered one of the most polluted cities globally due to the historical mining of lead (Pb) and Zinc (Zn) (Blacksmith Institute, 2013). Mining activities between 1902 and 1994 produced approximately 0.8 Mt and 1.8 Mt of Pb and Zn, respectively (Kamona and Friedrich, 2007). After nearly 90 years of operations without any environmental regulations, mining activities ceased in 1994 due to the depletion of the ore body. During the active period of the mine, huge stockpiles of mine wastes were disposed of and left unattended. Therefore, dust generation and transportation of potentially toxic elements (PTEs) from Kabwe mine wastes (KMW) to the surrounding environment was inevitable.

The PTEs can be accessed through inhalation, intentional or accidental ingestion of contaminated soil (Bello et al., 2016, Yabe et al., 2015). Depending on age groups, pica behavior is higher in children than adults because of their hand-to-mouth etiquette (Ljung et al., 2006, Yabe et al., 2015). The U.S. Environmental Protection Agency (EPA) estimates that a typical child up to 84 months can swallow 100 mg of contaminated soil/day (EPA, 2002). A study by Toyomaki et al. (2018) on the infants of Kabwe showed high Pb contents in their feces with an overall average value of 39.2 mg/kg. Bose-O'Reilly et al. (2018) and Yabe et al. (2020) also found that the children within the vicinity of the mine area of Kabwe contained high blood lead levels (BLLs) (BLLs > 5 µg/dL). Since children are the most affected, one potential exposure source of Pb intoxication for the children are school playgrounds soils (SPs).

Most of the playfields in Zambia are characterized by bare land and insufficient lawn maintenance. Therefore, there are several exposure pathways in which the PTEs can enter the body from the SPs, i.e., ingestion or inhalation of soil settled on play equipment or dust adhered to hands, fingers, or clothes (Jin et al., 2019, Peng et al., 2019). Subsequent exposure to such environment may lead to the uptake of PTEs into the respiratory and digestive systems, leading to the absorption of Pb into the bloodstream.

Elevated blood Pb is detrimental to human health and may cause severe nervous system problems, retardation, behavioral disorder and formation of porous bones due to substitutions (Pb apatite's) inside the bones (Yabe et al., 2015).

However, detecting high contents of PTEs in the soil, in particular, Pb and Zn, does not necessarily mean the high risk of contaminants in the environment or bioavailability into the body. Instead, this depends on the leachability of the heavy metals under various environmental conditions (Yan et al., 2020) The bioaccessible and bioavailable Pb and Zn in the soil depends on the binding and mineralogical forms in which they exist (Huyen et al., 2019, Tabelin et al., 2020). Thus, understanding their specific characteristics in the binding states leads to their bioaccessibility in the soil (Tabelin et al., 2018). Therefore, the purpose of this study was to determine the extent of pollution, leachability, the partitioning of Pb and Zn and the influence of distance from the mine site on the contents of Pb and Zn in the SPs, because the playgrounds might be a potential source of Pb intoxication for the children of Kabwe.

2.2 Materials and Methods

2.21 Site description and sampling location

A total of 8 soil samples were collected from a community ground in Kasanda area (S1), Makululu primary school (S2), Malumbo community ground (S3), Makululu day secondary (S4), Makululu day secondary garden (S5), David Ramushu secondary school (S6), David Ramushu secondary school garden (S7), and Kebar Christian academy (S8). Using a stainless-steel hand shovel, soil samples were collected from topsoil (about 5 cm deep) with 3 to 4 mixing points for each sample (Figure 3).

2.2.2 Soil characterization

Mineralogical and chemical properties of the soils were examined using pressed powders of the SPs (< 50 μm) and analysed using X-ray diffractometer (XRD) (MultiFlex, Rigaku Corporation, Tokyo, Japan) and X-ray fluorescence spectrometer (XRF) (Spectro Xepos, Rigaku Corporation, Tokyo, Japan), respectively. The SPs' particle size distribution was analyzed using the laser diffraction (Microtrac® MT3300SX, Nikkiso Co. Ltd., Osaka, Japan). The total organic carbon content was calculated by the difference

between total carbon content and inorganic carbon content measured by a total carbon analyzer with a solid sample combustion unit (TOC-VCSH-SSM-5000A, Shimadzu Corporation, Kyoto, Japan).

2.2.3 Determination of pollution indices

Two pollution indices were employed to calculate the extent of contamination in the SPs, i.e., geo-accumulation index (*Igeo*) and enrichment factor (*EF*). The *Igeo* quantifies the degree of anthropogenic contamination. The index was introduced by Muller. (1969), given by the following equation.

$$Igeo = \log_2(Cn/1.5Bn)$$

where, *Cn* is the content of an examined element in the SPs and *Bn* is the background value of the element in the studied area. This study selected the median soil background values in Sub-Sahara Africa (Towett et al., 2015). The value of 1.5 is a constant introduced to normalize the variances in background levels. Seven categories based on the level of contamination are classified as: class 0,uncontaminated ($Igeo < 0$); Class 1, uncontaminated to moderately contaminated ($0 < Igeo < 1$); Class 2, moderately contaminated ($1 < Igeo < 2$); Class 3, moderately to heavily contaminated ($2 < Igeo < 3$); Class 4, heavily contaminated ($3 < Igeo < 4$); Class 5, heavily to extremely contaminated ($4 < Igeo < 5$); and Class 6, extremely contaminated ($Igeo > 5$).

The *EF* differentiates between metals originating from human activities and natural processes. The *EF* was calculated as the ratio of the content of the metal in the sample to the content of the same metal in the earth crust using the modified formula from Buat-Menard and Chesselet. (1979), as shown below:

$$EF = (Mx*Tib)/(Mb*Tix)$$

where, *Mx* is the content of the measured sample, *Tib* is the background content of titanium (Ti) in the earth crust. The *Mb* is the background content of the targeted element in the earth crust, while *Tx* is the measured content of the reference value in the sample. The earth crust content values were taken from Turekian and Wedepohl. (1961). The calculated values were based on the classification of enrichment as: deficiency to minimal enrichment ($EF < 2$); moderate enrichment ($2 < EF < 5$); significant enrichment ($5 < EF$

< 20); very high enrichment (20 < *EF* < 40); and extremely high enrichment (*EF* > 40) (Sutherland et al., 2000).

2.2.4 Geochemical modeling and multivariant statistical Analysis

PHREEQC; Version 3, United States Geological Survey, Sunrise Valley Drive Reston, USA, was used to calculate the saturation indices (*SIs*) for the possible mineral phases controlling the release and retention of Pb and Zn in the SPs (Parkhurst and Appelo 1999). The thermodynamic properties were taken from the MINTEQ.V4.DAT database. Principal component analysis (PCA) was used for finding the correlations between the metal content or metal ion concentration and several environmental leaching conditions.

2.2.5 Batch leaching experiments

The batch leaching experiments were conducted by mixing 15g of soil sample and 150 mL of deionized (DI) water in a 300-mL Erlenmeyer flask followed by lateral reciprocating shaking speed of 200 rpm for 6 h. After the predetermined shaking time, the pH, oxidation-reduction potential (ORP) and electrical conductivity (EC) were measured followed by centrifugation of the suspension using a centrifuge (Sigma 3K30 laboratory centrifuge, Osterode, Germany) for 30 min at a speed of 3,500 rpm. The leachates from the experiments were collected by filtration through 0.45 Millex® filters (Merck Millipore, Burlington, MA, USA). The leachates were preserved by 1% nitric acid (HNO_3) before chemical analysis to maintain the target elements in dissolved forms. For accuracy and precision, all batches were performed in triplicates. The concentrations of major ions were then analyzed by inductively coupled plasma atomic emission spectroscopy (ICP-AES) (ICPE-9000, Shimadzu Corporation, Kyoto, Japan) (margin of error = ± 2~3%, determination limit 0.01-0.001 mg/L). All the chemicals used for conducting the experiments were reagent grade (Wako Pure Chemical Industries Ltd. Osaka, Japan).

2.26 Sequential extraction

The sequential extraction experiment was based on the earlier works of Tessier et al. (1979) and modifications of the procedure by Marumo et al. (2003). The procedure partitions Pb and Zn into five phases: (1) exchangeable, (2) carbonates, (3) iron and

manganese oxides, (4) organic matter and sulfide minerals, and (5) residual. The extraction procedure are summarized in Table 1. The extraction was done on 1g of SPs sample (< 2 mm) mixed with a predetermined volume of the extractant for each step. The leachate was separated from the residue by centrifugation of the suspension at 3,000 rpm for 30 min. Between each step, the residue was washed with 20 ml of DI water, which was combined with the leachate of the extraction step and diluted to 50 ml. The diluted solution was filtrated through 0.45-μm Millex® filters and kept in polypropylene bottles before chemical analysis. The samples were analyzed using inductively coupled plasma mass spectrometry (ICP-MS) (ICAP Qc, Thermo Fisher Scientific, Waltham, MA, USA).

Table 1. Procedure for the determination of the solid-phase partitioning of Pb and Zn

Phase	Extractant	L/S ratio (mL/g)	Temperature (°C)	Duration (h)	Speed (rpm)	Extracted phase
1	1 M $MgCl_2$ at pH 7	20/1	25	1	200	Exchangeable
2	1 M CH_3COONa at pH 5	20/1	25	5	200	Carbonates
3	0.04 M $NH_2OH{\cdot}HCl$ in 25% acetic acid at pH 5	20/1	80	5	120	Reducible
4	0.04 M $NH_2OH{\cdot}HCl$ in 25% acetic acid; 30% H_2O_2; 0.02 M HNO_3	36/1	80	5	120	Oxidizable
5	60% HNO_3	20/1	120	1		Residue

2.3 Results

2.3.1 Chemical composition and mineralogy of SPs

Table 2 illustrates the major chemical composition, total organic carbon (TOC) and trace elements (Pb and Zn) of the SPs. The samples were mainly dominated with SiO_2 (56.1-83.7 wt. %), Al_2O_3 (6.4-29.7 wt. %), and Fe_2O_3 (2.2-7.6 wt. %). The TOC for the samples ranged from 0.3 to 5 wt. %. The SPs were classified according to the United States Department of Agriculture (USDA) soil classification, as either sandy loam (S1, S5, S6, and S7), silt loam (S3, S4, and S8), or loam (S2) (Table 3). High contents of trace elements of Pb (265-3,320 mg/kg) and Zn (359-2,600 mg/kg) were observed in the SPs. Although Pb- and Zn-bearing minerals could not be detected in the samples (Figure 4), possible mineral phases might be attributed to anglesite ($PbSO_4$), and zinkosite ($ZnSO_4$)

(Tangviroon et al., 2020). The contents of Pb and Zn are much higher than the average background contents in Sub-Sahara Africa; Pb (37 mg/kg) and Zn (29 mg/kg) (Towett et al., 2015).

Table 2. Chemical composition of the major components and the trace elements in the school playground soils (SPs).

	SPs							
	S1	S2	S3	S4	S5	S6	S7	S8
SiO_2 (wt.%)	56.4	56.1	72.2	67.7	60.7	69.9	75.4	83.7
TiO_2 (wt.%)	0.9	1.6	0.8	1.4	1.0	1.0	1.3	1.0
Al_2O_3 (wt.%)	22.8	29.7	16.6	23.9	15.9	8.5	15.2	6.4
Fe_2O_3 (wt.%)	7.2	4	7.6	6.2	6.9	6.2	4	2.2
MnO (wt.%)	0.54	0.10	0.10	0.06	0.24	0.17	0.11	0.09
MgO (wt.%)	0.8	1.9	1.2	2.8	2.3	0.9	1	0.6
CaO (wt.%)	0.3	0.6	1.2	0.1	2.2	2	0.7	0.8
Na_2O (wt.%)	<0.1	<0.1	<0.1	<0.1	<0.1	<0.1	<0.1	<0.1
K_2O (wt.%)	0.9	0.8	1.1	1.1	0.7	0.7	1.5	0.7
P_2O_5 (wt.%)	0.26	0.14	0.17	0.08	0.06	0.12	0.26	0.24
S (wt.%)	0.2	0.07	0.07	0.05	0.06	0.2	0.15	0.93
TOC (wt.%)	2.46	1.86	2.79	0.52	0.33	0.77	1.55	5.02
Pb (mg/kg)	3,320	1,080	1,070	265	633	863	1,770	3,170
Zn (mg/kg)	2,600	1,990	750	359	399	1,370	1,840	2,090

Table 3. A brief description of the type of soil samples collected: Particle size distribution into clay, silt, and sand according to the United States Department of Agriculture for the size groups of mineral particles (USDA, 1987).

Sample	Location	Type of soil	Clay% (< 2 µm)	Silt% (2-50 µm)	Sand% (> 50 µm)
S1	Community ground in Kasanda	Sandy loam	2.51	47.9	49.6
S2	Makululu primary school	Loam	8	47.8	44.2
S3	Malumbo community ground	Silt loam	1.38	51.2	47.5
S4	Makululu day secondary	Silt loam	0.86	53.4	45.7
S5	Makululu day secondary garden	Sandy loam	0.42	37.2	62.3
S6	David Ramushu secondary school	Sandy loam	0	39.0	61.0
S7	David Ramushu secondary school garden	Sandy loam	0	43.8	56.2
S8	Kebar Christian academy	Silt loam	0.04	55.9	44.1

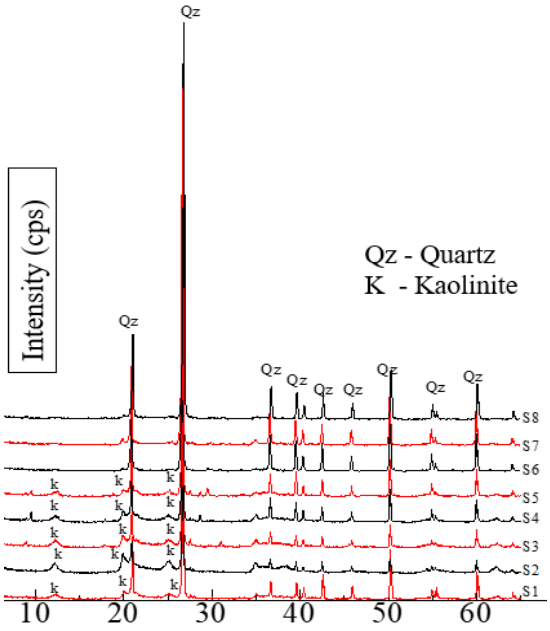

Figure 4. shows XRD patterns of the SPs.

Table 4 shows PCA multivariant correlations in the SPs using variables for the chemical compositions. The PCA 1, PCA 2, and PCA 3 accounted for 82% of the total chemical composition of the SPs. The PCA 1 showed that the Pb and Zn were associated with TOC and S with a 42% variance. This means that Pb and Zn had a close relationship with these chemical components in the SPs. PCA 2 and PCA 3 accounted for 21 and 19%, respectively. PCA 3 was mainly attributed to the geogenic chemical components (CaO, Fe_2O_3, and MnO) controlling the characteristics of the SPs such as pH, and release, and retention of Pb and Zn.

Table 4. Principal component analysis (PCA) for the chemical composition of the SPs, including total variance, eigenvalue, and cumulative frequency.

	PCA1	**PCA2**	**PCA3**
SiO_2 (wt.%)	0.24	-0.35	-0.31
Al_2O_3 (wt.%)	-0.22	**0.49**	-0.04
Fe_2O_3 (wt.%)	-0.24	-0.01	**0.44**
MnO (wt.%)	0.07	0.25	**0.55**
MgO (wt.%)	-0.37	0.04	-0.17
CaO (wt.%)	-0.09	-0.47	**0.25**
K_2O (wt.%)	-0.02	0.21	-0.25
P_2O_5 (wt.%)	0.37	0.23	0.02
S (wt.%)	**0.36**	-0.18	-0.12
TOC (wt.%)	**0.37**	-0.01	-0.07
Pb (mg/kg)	**0.39**	0.19	0.16
Zn (mg/kg)	**0.32**	**0.33**	0.08
Eigenvalue	5.47	2.68	2.45
Variance (%)	42.0	20.6	18.8
Cumulative	42.0	62.6	81.5

Table 5 shows the Pearson correlation matrix for the chemical composition of the SPs. A significant correlation between TOC and S were observed ($r = 0.8$, $p < 0.05$). The Pb showed high correlations with TOC ($r = 0.8$, $p < 0.05$) and S ($r = 0.7$, $p < 0.05$). On the other hand, Zn showed lower correlation with TOC ($r = 0.6$, $p > 0.05$) and S ($r = 0.4$, $p < 0.05$).

Table 5. Pearson correlation matrix for chemical composition for the soil samples. Marked correlation is significant at $p < 0.05$

	SiO_2 (wt.%)	TiO_2 (wt.%)	Al_2O_3 (wt.%)	Fe_2O_3 (wt.%)	MnO (wt.%)	MgO (wt.%)	CaO (wt.%)	K_2O (wt.%)	P_2O_5 (wt.%)	S (wt.%)	TOC (wt.%)	Pb (mg/kg)	Zn (mg/kg)
SiO_2 (wt.%)	1.0												
TiO_2 (wt.%)	-0.2	1.0											
Al_2O_3 (wt.%)	-0.8	0.6	1.0										
Fe_2O_3 (wt.%)	-0.5	-0.5	0.2	1.0									
MnO (wt.%)	-0.6	-0.4	0.2	0.5	1.0								
MgO (wt.%)	-0.4	0.5	0.6	0.3	-0.3	1.0							
CaO (wt.%)	0.0	-0.4	-0.5	0.3	0.0	-0.1	1.0						
K_2O (wt.%)	0.2	0.2	0.2	0.0	-0.2	0.0	-0.4	1.0					
P_2O_5 (wt.%)	0.3	-0.2	-0.2	-0.4	0.3	-0.8	-0.4	0.4	1.0				
S (wt.%)	**0.7**	-0.3	-0.6	-0.7	-0.1	-0.6	-0.1	-0.3	0.5	1.0			
TOC (wt.%)	0.5	-0.3	-0.3	-0.5	0.0	-0.7	-0.3	-0.1	0.7	**0.8**	1.0		
Pb (mg/kg)	0.2	-0.4	-0.2	-0.4	0.5	-0.8	-0.4	-0.1	0.9	**0.7**	**0.8**	1.0	
Zn (mg/kg)	0.0	0.0	0.0	-0.5	0.4	-0.7	-0.4	0.0	0.8	0.4	**0.6**	**0.8**	1

2.3.2 The Extent of pollution and particle size distribution of the SPs

Table 6 summarizes *Igeo* and *EF*. The SPs from S1, S3, S7 and S8 showed 'extremely high enrichment' of Pb (*EF* > 40). Meanwhile, S2, S5 and S6 had 'very high enrichment' of Pb (20 < *EF* < 40). The S4 had the lowest enrichment of Pb (5 < *EF* < 20, indicating a significant enrichment). However, only S1 showed 'very high enrichment' for Zn (20 < *EF* < 40), while S2, S3, S6 and S7 indicated 'significant enrichment' of Zn (5 < *EF* < 20). The order of enrichment followed S1 > S8 > S3 > S7 > S6 > S2 > S5 > S4 for Pb and S1 > S8 > S7 > S6 > S2 > S3 > S5 > S4 for Zn. The *Igeo* for SPs indicated that S1, S2, S3, S6, S7, and S8 were 'extremely contaminated' with Pb (*Igeo* > 5). The S4 and S5 were heavily (3 < *Igeo*< 4) and heavily to extremely (4 < *Igeo* < 5) contaminated with Pb, respectively. Meanwhile, S1, S2, S6, S7 and S8 were 'extremely contaminated' with Zn. The order of contamination followed S1, S8 > S7 > S3, S2 > S6 > S5 > S4 for Pb and S1 > S8, S2 > S7 > S6 > S3 > S5 > S4 for Zn. The pollution indices show that the SPs were highly enriched and contaminated with PTEs.

Table 6. Calculated pollution indices with the total average value across the playgrounds.

Playgrounds	Enrichment factor (*EF*)		Geoaccumulation Index (*Igeo*)	
	Pb	Zn	Pb	Zn
S1	141.4	23.4	5.9	5.9
S2	25.4	9.9	4.3	5.5
S3	53.2	7.8	4.3	4.1
S4	7.5	2.1	2.3	3.0
S5	23.2	3.1	3.5	3.2
S6	32.1	10.7	4.0	5.0
S7	50.3	11.1	5.0	5.4
S8	124.9	17.3	5.8	5.6
Average	**57.3**	**10.7**	**4.4**	**4.7**

Figure 5 shows the particle size distribution of the SPs and predominate mining residual materials, i.e.,Zinc leach plant residues (ZLPRs). The residues have fine particles (< 6 µm at 10 % effective diameter (D_{10})). Particles (< 20 µm) are likely to become aerosol from the mine wastes; consequently, finer particles might be transported further (Kok et al., 2012). This could be the reason why the samples at S2, the furthest site from the mine

wastes, recorded ‘very high enrichment’ of Pb. In addition, Nakamura et al. (2021) simulated the deposition of aerosols particles at S2 and the results suggested that prevailing winds in the northwest, north-northwest, and north direction from the mine wastes influenced the deposition of smaller particles to the area.

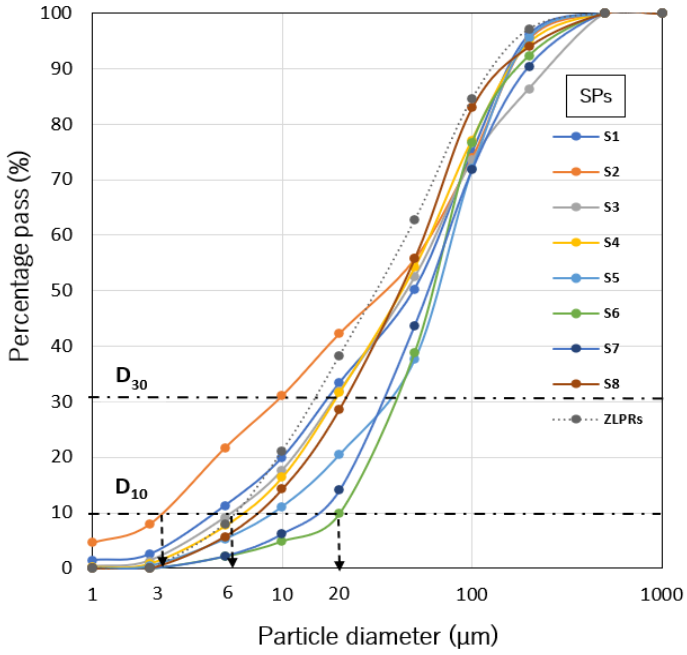

Figure 5. Particle size distribution of SPs and the zinc leach plant residues (ZLPRs) with their 10% and 30% diameters D_{10} and D_{30}.

2.3.3. Leaching characteristics of SPs

Figure 6 shows the leachate characteristics of the SPs based on the standard leaching tests. The leachates were compared with the standards of Zambia Bureau for drinking water quality (ZS.190.2010). The quality prescribes requirements for drinking water suitable for human consumption. The SPs from S4, S5, and S6 had no leachable Pb, while S1, S2, S3, S7, and S8 had leaching concentrations of Pb above the permissible limit for drinking water in Zambia (Pb < 0.01 mg/L) (Figure 6a). Meanwhile, Zn was within the tolerable limit for all the SPs (Zn < 3 mg/L). The pH of all the SPs ranged from slightly acidic to alkaline conditions (pH 6.2–8.2). The pH values of the leachates from S1, S4, S5, and S6 exceeded the Zambian drinking water standard (pH 6.5–8.0), while those from S2, S3, S7, and S8 were within the permissible limits (Figure 6b).

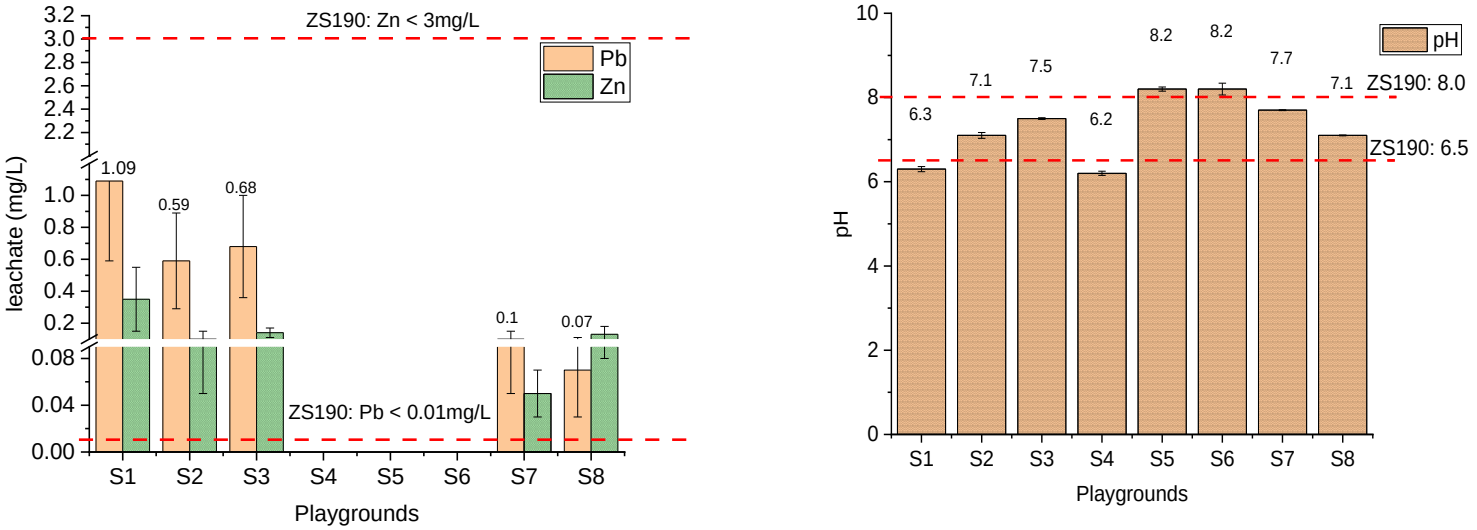

(a) (b)

Figure 6. Leachate characteristics for the SPs: (a) water-soluble Pb and Zn (b) pH. The dotted line represents permissible limits for drinking water standards in Zambia.

Table 7 shows the results from PCA analysis using the leachate concentration. PCA 1 and PCA 2 accounted for 79% of the total variance, with high loadings of Al, Si, Fe, Pb, SO_4^{2-}, pH, EC, Eh, Mg and Zn. The PCA loadings of alkalinity, positive pH, and Ca in PCA 3 (17% variance) indicate the chemical components controlling the buffering effects of the SPs. This is consistent with geogenic CaO in PCA 3 for the chemical composition of the SPs. The high loadings of SO_4^{2-}, Mg, EC, and Eh in PCA 2 accounted for 27% of the co-existing ions controlling the EC of the leachate in SPs.

Table 7. Principal Component Analysis (PCA) for water-soluble Pb and Zn, including total variance, eigenvalue, and cumulative frequency.

	PCA 1	PCA 2	PCA 3
pH	-0.24	**-0.31**	**0.38**
Eh (mV)	0.2	**0.42**	-0.29
EC (mS/cm)	-0.27	**0.36**	0.24
alkalinity	-0.24	-0.29	**0.38**
Ca (mg/L)	-0.34	0.12	**0.32**
Si (mg/L)	0.36	-0.02	0.29
Fe (mg/L)	**0.34**	-0.03	**0.32**
Al (mg/L)	**0.35**	-0.04	0.31
SO_4^{2-} (mg/L)	-0.2	0.46	0.16
Pb (mg/L)	**0.36**	0.09	0.25
Zn (mg/L)	**0.28**	0.29	0.25
Mg (mg/L)	-0.19	0.44	0.19
Eigenvalue	6.19	3.26	2.01
Variance (%)	52	27	17
Cumulative	52	79	96

2.3.4. Partitioning of Pb and Zn in the SPs

The sequential extraction patterns of Pb and Zn are shown in Figure 7. The solid-phase partitioning of Pb in the SPs ranged from 0.3 to 21% for the exchangeable fraction, weak acid soluble (17 to 42%), reducible (20 to 43%), oxidizable (16 to 33%), and residue (4 to 20%) (Figure 7a). Meanwhile for Zn, exchangeable (0.4 to 23%), weak acid soluble (13 to 33%), reducible (13 to 45%), oxidizable (9 to 23%) and residue (10 to 51%) (Figure 7b). The Pb in the SPs was mainly bound with carbonates, reducible and oxidizable phases while Zn showed strong association with reducible and residue fractions.

Figures 8 and 9 illustrate the leachable water-soluble (Pb and Zn) relationship with the exchangeable, labile phases (exchangeable + carbonates + Fe/Mn oxides) and total content. The water-soluble Pb showed a strong correlation with exchangeable phase (r = 0.8), labile phase (r = 0.6), and a lower correlation with the total content (r = 0.5). The correlation for the water-soluble Zn showed r = 0.9 with the exchangeable phase, r = 0.5 with the labile phase and r = 0.6 with the total content. The correlations certainly indicate the close relationship between the water-soluble Pb and Zn with the exchangeable phase.

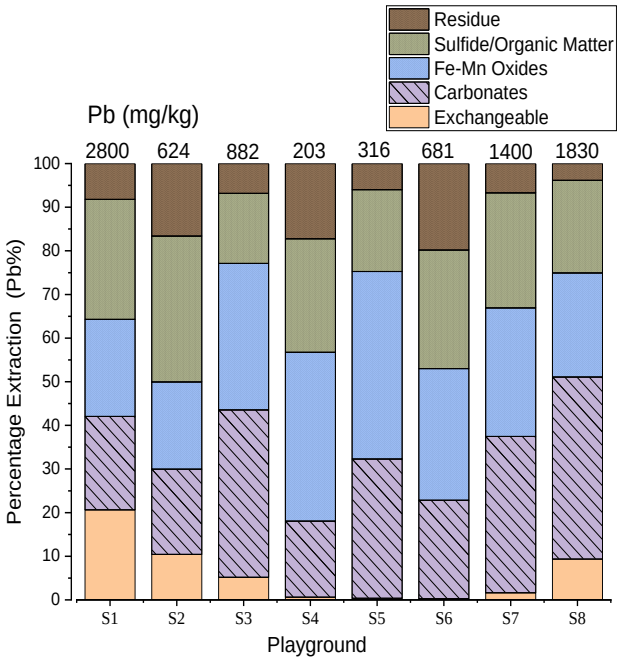

(a)

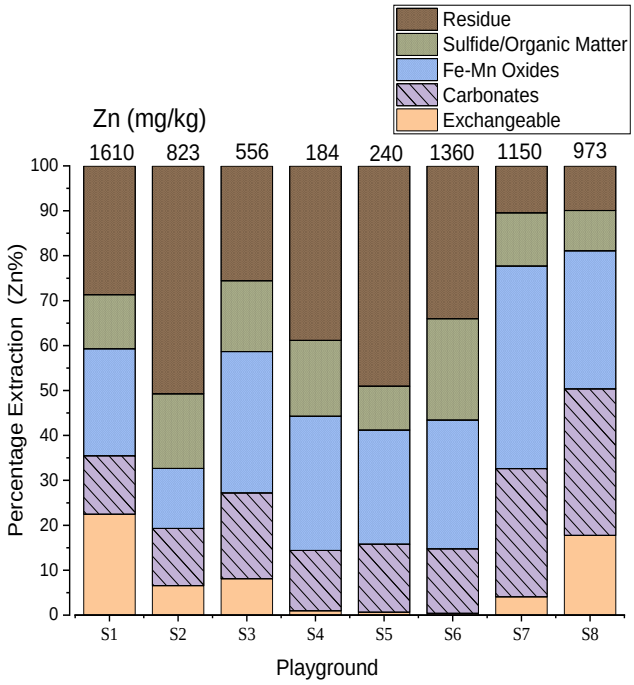

(b)

Figure 7. Solid-phase partitioning of Pb (a) and Zn (b) in SPs. The values on top of each sample represent the total content (mg/kg) from the extraction of the five phases. The phases are expressed in percentage of the total content.

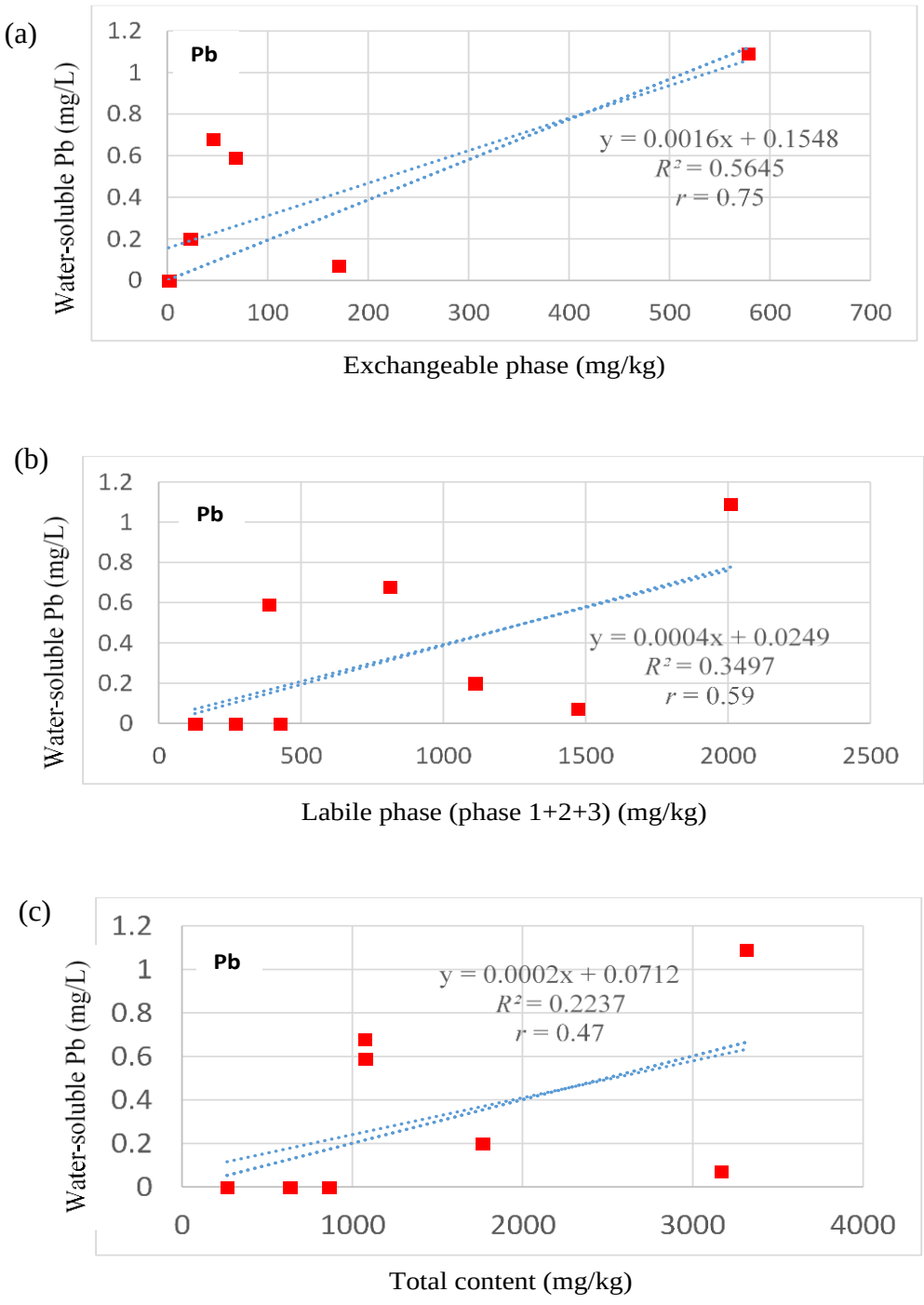

Figure 8. Relationship between water-soluble Pb with (a) exchangeable phase (b) labile phase 1+2+3 and (c) total content

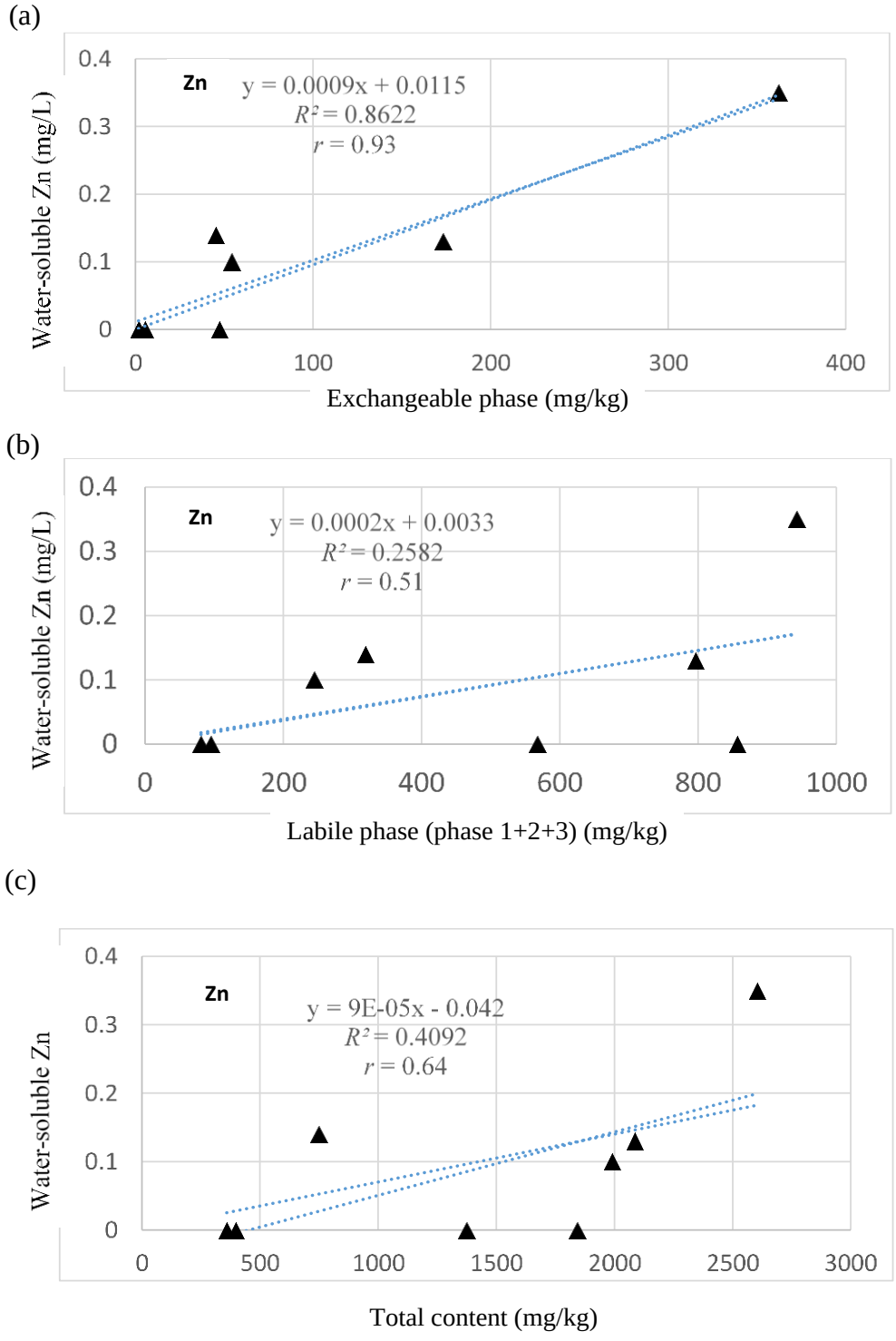

Figure 9. Relationship between water-soluble Zn with (a) exchangeable phase (b) labile phase 1+2+3 and (c) total content

.

2.3.5 The Distance of SPs from the KMWs

Figure 10 shows the trend of the total content, exchangeable phase, and the water-soluble Pb and Zn for each SPs site with the distance from the Kabwe mine wastes (KMWs). The S1 and S8 are the nearest sites to the KMWs. Consequently, they had the highest contents of Pb and Zn, with S1 having 3,320 mg/kg for Pb and 2,600 mg/kg for Zn, while S8 records 3,170 mg/kg for Pb and 2,090 mg/kg for Zn (Figure 5a). The trend was similar to water-soluble and exchangeable phases (Figures 10 b, c). There was a noticeable decrease as moving away from the KMWs.

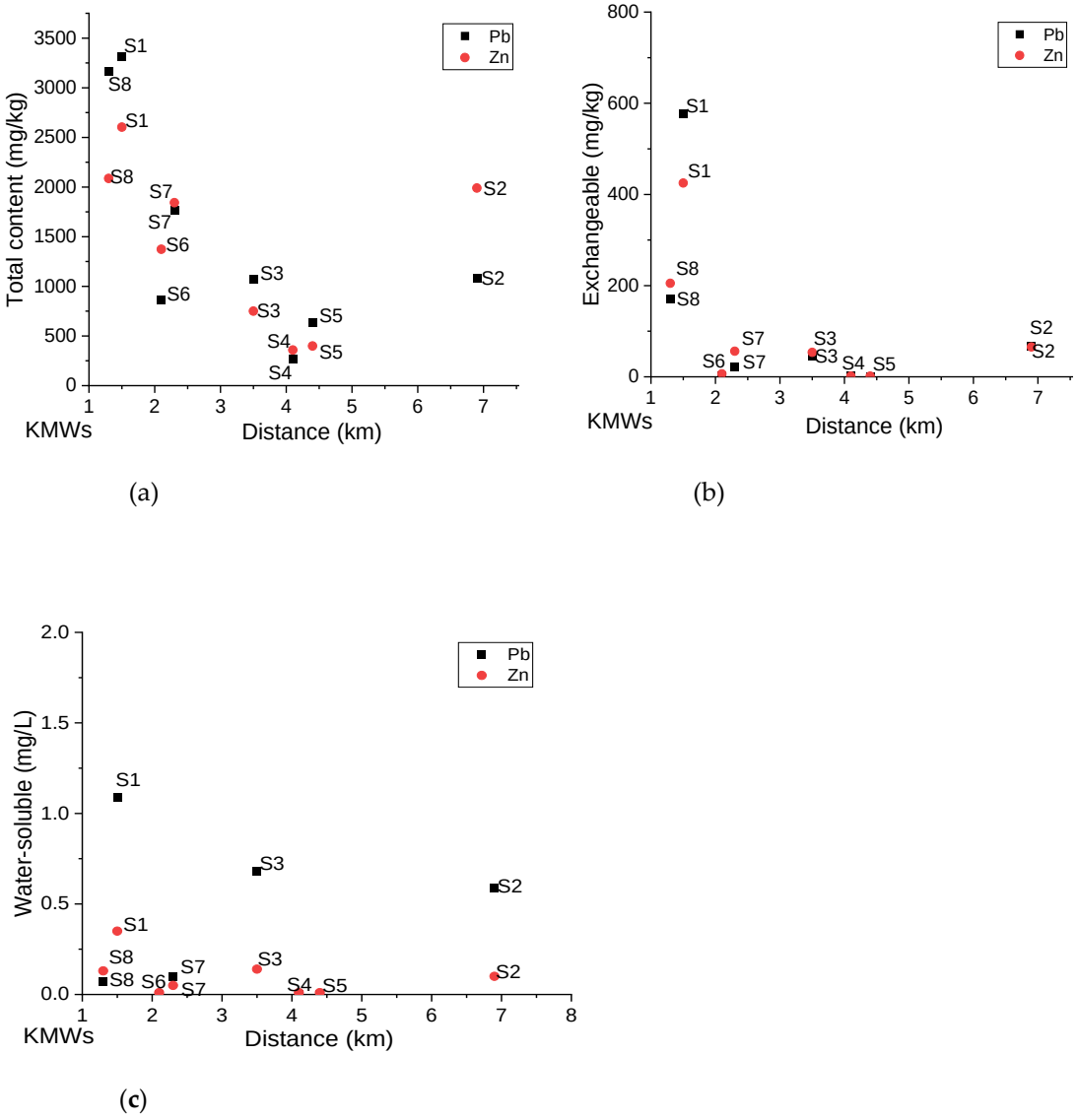

Figure 10. The distribution of Pb and Zn with the distance of each playground from Kabwe Mine Wastes (KMWs): (a) contents (XRF), (b) exchangeable and (c) water-soluble.

3. Discussion

The SPs have exceptionally high contents of Pb and Zn. Soil contamination in the SPs might be attributed to the deposition of aerosol particles to surrounding soils from the KMWs. Nakamura et al. (2021) confirmed that the contents of Pb generally increased with the amount deposited; also, the Pb content in the SPs and the simulated amount of

deposition decreased with distance from the source. This is consistent with the high enrichment and contamination of Pb in the soils near the mine area (S1 and S8). The results of the substantial enrichment in S1 and S8 agreed with the profound intensity of contamination in the SPs near the KMWs.

The discrepancies in the contents and leaching of Pb and Zn in the SPs might be attributed to the volume of aerosols deposited, particle size distribution and environmental conditions controlling the mobilities of the PTEs. The mobility of PTEs such as Pb and Zn in groundwater, mine tailings, and contaminated soils is extensively influenced by the pH, precipitation, redox conditions, and adsorption/desorption reactions (Tabelin and Igarashi., 2009). However, the overall enrichment of Pb and Zn were generally high in all the SPs. In comparison with other playgrounds of different cities in the world, the contents of Pb and Zn from Kabwe SPs were higher than those of Warsaw and Bydgoszcz, Poland (Pb up to 167 mg/kg, Zn up to 57.4 mg/kg (Różański et al., 2018), Beijing, China (Pb up to 207.5 mg/kg, Zn, up to 196.9 mg/kg (Chen et al., 2005), Ibadan, Nigeria (Pb up to 58 mg/kg, Zn up to 460 mg/kg (Akinwunmi et al., 2017) and country parks, Hong Kong (Pb up to 124 mg/kg, Zn up to 136 mg/kg (Lee et al., 2006)

Figure 6a showed that the Pb in the leachates from S1, S2, S3, S7, and S8 were above the permissible limit for drinking water in Zambia. Water consumption from such an environment may be detrimental to human health because some communities in Kabwe rely on groundwater from boreholes. The release of Pb from the SPs may be attributed to sulfide oxidation (Tabelin et al., 2020). This is explained by the SO_4^{2-} in PCA 2 for the leachate concentration. The high loadings of SO_4^{2-}, EC, and Eh suggest the sulfide minerals oxidation in the SPs, even though they were not detected by XRD. Silwamba et al. (2020) also pointed out that in the leaching system for ZLPR from the Kabwe dump site, the SO_4^{2-} was attributed to the soluble minerals phases, anglesite ($PbSO_4$), zinkosite ($ZnSO_4$), and gypsum $CaSO_4{\cdot}2H_2O$. The anglesite and zinkosite are known to be the exchangeable products of sulfide oxidation in minerals containing Pb and Zn.

Table 8 shows the PHREEQC simulation for the possible mineral phases that affected the release and retention of Pb and Zn in the SPs. The results showed that the *SIs* for $CaSO_4.2H_2O$ (−3.45 to −1.55) and $PbSO_4$ (−2.41 to −1.43) implied the dissolution of

these mineral phases,which suggests that the release Pb in the SPs was as a result of dissolution of $PbSO_4$. However, the *SIs* of goethite ($Fe(OH)_3$; 4.58 to 7.94) and those of ferrihydrite (FeOOH; 1.85 to 5.22) showed that precipitation was thermodynamically favoured after leaching. This explains why no leachable Pb, and Zn were detected in S4, S5 and S6, meaning that the available Pb and Zn in the SPs might have been redistributed and adsorbed with hydrous ferric oxides (HFOs). The HFOs have an excellent affinity for elements such as Pb, Cu, Cd, Zn, Ni, and metal oxyanions such as Cr, Sb, and As (Shi et al., 2020, Trivedi et al., 2020).

Table 8. Saturation indices (*SI*) of selected mineral phases controlling the release and retention of Pb and Zn in the selected SPs.

	$CASO_4{\cdot}2H_2O$	$PbSO_4$	FeOOH	$Al(OH)_3$	$Fe(OH)_3$
SPs	Gypsum	Anglesite	Ferrihydride	Gibbsite	Goethite
S1	-2.93	-1.43	4.05	4.76	6.77
S2	-3.45	-2.33	4.58	4.39	7.30
S3	-3.15	-2.19	5.22	4.05	7.94
S7	-2.51	-2.41	5.07	3.61	7.79
S8	-1.55	-2.03	1.85	3.1	4.61

SI > 0: Saturated, *SI* < 0: Unsaturated

Fractionation of Pb by sequential extraction confirmed the strong associations between Pb with the reducible and oxidizable phases. The strong associations of Pb with reducible phase, entailed that the Pb was relatively stable after deposition and might have been attributed to the weathering of galena (PbS) (Prathumratana e al., 2020). The Pb bound to the oxidizable phases (sulfide/organic) was higher than Zn. The results agree with the correlations of Pb with S and TOC from the chemical composition of the SPs. The strong correlations of Pb with TOC means that some of the Pb were retained with the organic phases (Khan et al., 2016). Baran et al. (2019) also highlighted the strong correlations of Pb, Cu, Ni, and Cr with TOC in the organic phase.

The mobile fractions for the labile phases (exchangeable + carbonates + Fe/Mn oxides) for Pb and Zn were notably high for all the SPs. Generally, it is typically assumed that the greater the labile percentage, the greater the potential for bioavailability in the body (Sethurajan et al., 2016). Therefore, the high bioaccessible fractions of PTEs in the

labile phases significantly increase the bioaccessibility of the ingested PTEs, thereby posing a serious threat to the respiratory and digestive systems for the children because a substantial amount of PTEs might be absorbed into the bloodstream.

The correlations between the leachable water-soluble Pb and Zn with the exchangeable, labile phases and the total content suggests that the release of Pb and Zn into the environment from the SPs was mainly attributed to the exchangeable phase and not so much from the total content of Pb and Zn (Figures 8 and 9). In addition, the Pb bound to carbonate phase is usually influenced by the pH of the environment; for example, under gastric conditions, cerussite ($PbCO_3$) might significantly dissolve in the acidic conditions (Helser and Cappuyns., 2021), which increases the bioaccessibility of ingested PTEs. However, the present study could not identify the host minerals for the PTEs; electron microprobe analysis might be a possible approach to identifying the mineral phases (Vollprecht et al., 2020)

4 Conclusion

The leachability, solid-phase partitioning, and contamination assessment of the school playground soils near the mine area were evaluated. The anthropogenic contamination and enrichment of Pb and Zn in the SPs were traced back to the old mining activities. The playgrounds showed high enrichment of Pb and Zn. The Pb and Zn in the SPs were mainly bound with the exchangeable, carbonates, reducible and oxidizable phases. The labile phases' bioaccessible fractions of Pb and Zn were exceptionally high for all the playground soils. The results suggest that the SPs are potential sources of toxic elements for the children in Kabwe. Furthermore, the human health risk associated with inhalation/ingestion of toxic elements from the SPs is high. Therefore, revegetation, soil turning, and watering of the playgrounds to suppress dust generation could be short-term measures to reduce the high bioaccessibility of Pb and Zn in the playgrounds.

References

Akinwunmi, F., Akinhanmi, T.F., Atobatele, Z.A., Adewole, O., Odekunle, K., Arogundade, L.A., Odukoya, O.O., Olayiwola, O.M. and Ademuyiwa, O., 2017. Heavy metal burdens of public primary school children related to playground soils and classroom dusts in Ibadan North-West local government area, Nigeria. Environmental Toxicology and Pharmacology, 49, pp. 21-26.

Baran, A., Mierzwa-Hersztek, M., Gondek, K., Tarnawski, M., Szara, M., Gorczyca, O. and Koniarz, T., 2019. The influence of the quantity and quality of sediment organic matter on the potential mobility and toxicity of trace elements in bottom sediment. Environmental Geochemistry and Health, 41(6), pp. 2893-2910.

Bello, O., Naidu, R., Rahman, M.M., Liu, Y. and Dong, Z., 2016. Lead concentration in the blood of the general population living near a lead–zinc mine site, Nigeria: Exposure pathways. Science of the Total Environment, 542, pp. 908-914.

Blacksmith Institute and Green Cross Switzerland. 2013. Available online: https://www.worstpolluted.org/docs/TopTenThreats.pdf

Bose-O'Reilly, S., Yabe, J., Makumba, J., Schutzmeier, P., Ericson, B. and Caravanos, J., 2018. Lead intoxicated children in Kabwe, Zambia. Environmental Research, 165, pp. 420-424.

Buat-Menard, P. and Chesselet, R., 1979. Variable influence of the atmospheric flux on the trace metal chemistry of oceanic suspended matter. Earth and Planetary Science Letters, 42(3), pp. 399-411.

Chen, T.B., Zheng, Y.M., Lei, M., Huang, Z.C., Wu, H.T., Chen, H., Fan, K.K., Yu, K., Wu, X. and Tian, Q.Z., 2005. Assessment of heavy metal pollution in surface soils of urban parks in Beijing, China. Chemosphere, 60(4), pp. 542-551.

EPA, US. A Review of the Reference Dose and Reference Concentration Processes. Risk Assessment Forum. The Environmental Protection Agency: Washington, DC, USA, 2002.

Helser, J. and Cappuyns, V., 2021. Trace elements leaching from pbzn mine waste (plombières, belgium) and environmental implications. Journal of Geochemical Exploration, 220, p.106659.

Huyen, D.T., Tabelin, C.B., Thuan, H.M., Dang, D.H., Truong, P.T., Vongphuthone, B., Kobayashi, M. and Igarashi, T., 2019. The solid-phase partitioning of arsenic in unconsolidated sediments of the Mekong Delta, Vietnam and its modes of release under various conditions. Chemosphere, 233, pp. 512-523.

Jin, Y., O'Connor, D., Ok, Y.S., Tsang, D.C., Liu, A. and Hou, D., 2019. Assessment of sources of heavy metals in soil and dust at children's playgrounds in Beijing using GIS and multivariate statistical analysis. Environment International, 124, pp. 320-328.

Kamona, A.F. and Friedrich, G.H., 2007. Geology, mineralogy and stable isotope geochemistry of the Kabwe carbonate-hosted Pb–Zn deposit, Central Zambia. Ore Geology Reviews, 30(3-4), pp. 217-243.

Khan, B., Ullah, H., Khan, S., Aamir, M., Khan, A. and Khan, W., 2016. Sources and contamination of heavy metals in sediments of Kabul River: The role of organic matter in metals retention and accumulation. Soil and Sediment Contamination: An International Journal, 25(8), pp. 891-904.

Kok, J.F., Parteli, E.J., Michaels, T.I. and Karam, D.B., 2012. The physics of wind-blown sand and dust. Reports on Progress in Physics, 75(10), 106901.

Lee, C.S.L., Li, X., Shi, W., Cheung, S.C.N. and Thornton, I., 2006. Metal contamination in urban, suburban, and country park soils of Hong Kong: a study based on GIS and multivariate statistics. Science of the Total Environment, 356(1-3), pp. 45-61.

Ljung, K., Selinus, O. and Otabbong, E., 2006. Metals in soils of children's urban environments in the small northern European city of Uppsala. Science of the Total Environment, 366(2-3), pp. 749-759.

Marumo, K., Ebashi, T. and Ujiie, T., 2003. Heavy metal concentrations, leachabilities, and lead isotope ratios of Japanese soils. Shigen-Chihsitsu, 53,pp. 125–146.

Muller, G. 1969. Index of geo-accumulation in sediments of the Rhine River. GeoJournal, 2,pp. 108–118

Nakamura, S., Igarashi, T., Uchida, Y., Ito, M., Hirose, K., Sato, T., Mufalo, W., Chirwa, M., Nyambe, I., Nakata, H., Nakayama, S. and Ishizuka M., 2021. Evaluation of dispersion of Lead-Bearing Mine Wastes in Kabwe District, Zambia. Minerals, 11(8), 901.

Parkhurst, D.L. and Appelo, C.A.J., 1999. User's guide to PHREEQC (Version 2): A computer program for speciation, batch-reaction, one-dimensional transport, and inverse geochemical calculations. Water-Resources Investigations report, 99(4259), 312p.

Peng, T., O'Connor, D., Zhao, B., Jin, Y., Zhang, Y., Tian, L., Zheng, N., Li, X. and Hou, D., 2019. Spatial distribution of lead contamination in soil and equipment dust at children's playgrounds in Beijing, China. Environmental Pollution, 245, pp. 363-370.

Prathumratana, L., Kim, R. and Kim, K.W., 2020. Lead contamination of the mining and smelting district in Mitrovica, Kosovo. Environmental geochemistry and health, 42(3), pp. 1033-1044.

Różański, S.Ł., Kwasowski, W., Castejón, J.M.P. and Hardy, A., 2018. Heavy metal content and mobility in urban soils of public playgrounds and sport facility areas, Poland. Chemosphere, 212, pp. 456-466.

Shi, M., Min, X., Ke, Y., Lin, Z., Yang, Z., Wang, S., Peng, N., Yan, X., Luo, S., Wu, J. and Wei, Y., 2021. Recent progress in understanding the mechanism of heavy metals retention by iron (oxyhydr) oxides. Science of the Total Environment, 752, 141930.

Silwamba, M., Ito, M., Hiroyoshi, N., Tabelin, C.B., Fukushima, T., Park, I., Jeon, S., Igarashi, T., Sato, T., Nyambe, I., Chirwa, M., Banda, K.,Nakata, H.,Nakayama, S. and Ishizuka, M., 2020. Detoxification of lead-bearing zinc plant leach residues from Kabwe, Zambia by coupled extraction-cementation method. Journal of Environmental Chemical Engineering, 8(4), 104197.

Sutherland, R.A., Tolosa, C.A., Tack, F.M.G. and Verloo, M.G., 2000. Characterization of selected element concentrations and enrichment ratios in background and anthropogenically impacted roadside areas. Archives of Environmental Contamination and Toxicology, 38(4), pp. 428-438.

Tabelin, C.B., Igarashi, T., Villacorte-Tabelin, M., Park, I., Opiso, E.M., Ito, M. and Hiroyoshi, N., 2018. Arsenic, selenium, boron, lead, cadmium, copper, and zinc in naturally contaminated rocks: A review of their sources, modes of enrichment, mechanisms of release, and mitigation strategies. Science of the Total Environment, 645, pp. 1522-1553.

Tabelin, C.B., Silwamba, M., Paglinawan, F.C., Mondejar, A.J.S., Duc, H.G., Resabal, V.J., Opiso, E.M., Igarashi, T., Tomiyama, S., Ito, M. and Hiroyoshi, N., 2020. Solid-phase partitioning and release-retention mechanisms of copper, lead, zinc and arsenic in soils impacted by artisanal and small-scale gold mining (ASGM) activities. Chemosphere, 260, 127574.

Tessier, A., Campbell, G.C and Bisson, M., 1979. Sequential extraction procedure for the speciation of particulate trace metals. Anal. Chem. 51, pp. 844–851

Trivedi, P., Dyer, J.A., Sparks, D.L. and Pandya, K., 2004. Mechanistic and thermodynamic interpretations of zinc sorption onto ferrihydrite. Journal of Colloid and Interface Science, 270(1), pp. 77-85.

Towett, E.K., Shepherd, K.D., Tondoh, J.E., Winowiecki, L.A., Lulseged, T., Nyambura, M., Sila, A., Vågen, T.G. and Cadisch, G., 2015. Total elemental composition of soils in Sub-Saharan Africa and relationship with soil forming factors. Geoderma Regional, 5, pp. 157-168.

Toyomaki, H., Yabe, J., Nakayama, S.M., Yohannes, Y.B., Muzandu, K., Mufune, T., Nakata, H., Ikenaka, Y., Kuritani, T., Nakagawa, M, Choongo, K and Ishizuka, M., 2021. Lead concentrations and isotope ratios in blood, breastmilk and feces: Contribution of both lactation and soil/dust exposure to infants in a lead mining area, Kabwe, Zambia. Environmental Pollution, 286, 117456.

Turekian, K and Wedepohl, K., 1961. Distribution of the elements in some major units of the earth's crust. Geol. Soc. Am. Bull. 72, pp. 175–192

Vollprecht, D., Riegler, C., Ahr, F., Stuhlpfarrer, S. and Wellacher, M., 2020. Sequential chemical extraction and mineralogical bonding of metals from Styrian soils. International Journal of Environmental Science and Technology, 17(8), pp. 3663-3676.

Yabe, J., Nakayama, S.M., Nakata, H., Toyomaki, H., Yohannes, Y.B., Muzandu, K., Kataba, A., Zyambo, G., Hiwatari, M., Narita, D. and Yamada, D., 2020. Current trends of blood lead levels, distribution patterns and exposure variations among household members in Kabwe, Zambia. Chemosphere, 243, 125412.

Yabe, J., Nakayama, S.M., Ikenaka, Y., Yohannes, Y.B., Bortey-Sam, N., Oroszlany, B., Muzandu, K., Choongo, K., Kabalo, A.N., Ntapisha, J., Mweene, A and Ishizuka, M., 2015. Lead poisoning in children from townships in the vicinity of a lead–zinc mine in Kabwe, Zambia. Chemosphere, 119, pp. 941-947.

Yan, B., Xu, D.M., Chen, T., Yan, Z.A., Li, L.L. and Wang, M.H., 2020. Leachability characteristic of heavy metals and associated health risk study in typical copper mining-impacted sediments. Chemosphere, 239, 124748.

USDA,1987. https://www.wcc.nrcs.usda.gov/ftpref/wntsc/H&H/training/soilsother/soil-USDA-textural-class.pdf

Chapter 3

SOLUBILITY OF LEAD AND ZINC IN THE MINE RESIDUE MATERIALS FROM A LEGACY MINE IN KABWE, ZAMBIA: BIOACCESSIBILITY IN SIMULATED FLUIDS, SOLID-PHASE PARTITIONING, AND INFLUENCE ON SURROUNDING SOILS

3.1 Introduction

Mining activities come with economic development and rapid industrialization; however, environmental degradation is inevitable after decommissioning. The negative aspect may include the anthropogenic influence of the by-products. For example, the tailings, overburdened rocks, and slag heaps stand out with the most significant volume, carrying toxic elements. The risks of the toxic elements (TEs) depend on their partitioning, particle size, bioaccessibility, and bioavailability in the body (Li et al., 2021). Many researchers have reported the environmental and health implications of legacy mining activities (Abraham et al., 2018; Helser and Cappuyns, 2021; Reyes et al., 2021). In recent years, one old mining activity of global concern has been carried out in the town of Kabwe in Zambia, which had significant Pb-Zn deposits. The processing and mining activities ceased due to the depletion of the ore body (1902-1994), leaving tonnes of mine wastes. High Pb contents (> 1,000 mg/kg) have been reported predominantly in soils near the dumping site (Baieta et al., 2021, Kribek et al., 2019).

The probability of dermal contact, accidental ingestion, or inhalation of the mine wastes or contaminated soil with TEs by the residents in Kabwe is high. The Center for Disease Control and Prevention (CDC) has set a reference value for blood lead level (BLL) exposure (< 5 µg/dL). The children within the vicinity of the legacy Kabwe mine have constantly recorded high BLL (BLL > 10) (Bose-O'Reilly et al., 2018). The records certainly explain the impact of the historical mine on the BLL of the residents. Generally, elements (Ca, Mg, Fe, and Co) are essential for human consumption and may not have dentrimental effects when taken up in the right amounts. However, TEs (Pb, Ba, Cr, Cu, Mo, Se, and Zn) may be harmful, even when taken in lesser amounts. After ingestion or inhalation of mine wastes or contaminated soil, only a fraction of the TEs will become solubilized or bioaccessible in the gastric/lung fluids and be considered bioavailable.

Based on gastric/lung conditions, the TEs ingested from a contaminated site might be partial or soluble (Soltani et al., 2021)

The TEs solubility may provide necessary estimates of bioaccessibility (Weggeberg et al., 2019). Extraction in simulated fluids (SFs) constitutes a physiologically relevant yet simple and inexpensive method of assessing the bioaccessibility of TEs. Recently, complex solutions have been used to reproduce lung and stomach fluids that simulate the actual conditions of accidental inhalation and ingestion of TEs (Pelfrêne et al., 2017). The bioavailable Pb in the body depends on the amount of bioaccessible TEs reaching the bloodstream. Usually, the pH, adsorption/desorption, precipitation, redox reactions, and particle size distribution significantly affect the mobility of heavy metals, leading to their bioaccessibility (Tabelin et al., 2018). Therefore, in-vitro assays using lung and gastric fluids are employed to understand the risks and bioaccessible fractions from mine wastes/soils or sediments. Since the fate of inhaled particles is a function of their solubility in the lung/stomach, this study employed leaching experiments using SFs, i.e., artificial lysosomal fluid (ALF), gamble solution (GS), and phosphate-buffered saline (PBS) on inhalable dust (< 30 um) from Kabwe, Zambia. This study assessed the solubility and bioaccessibility of Pb and Zn in mining residual materials (MRM) and soil samples in SFs. The solubility and bioaccessible fractions were compared with hydrochloric acid (HC*l*) solution, mimicking stomach conditions from the intentional/accidental ingestion of MRM or contaminated soil samples. The study aimed to evaluate bioaccessible levels and potential exposure routes for human intoxication of Pb and Zn in the local people who have access to or live near the legacy mine in Kabwe, Zambia.

3.2 Materials and Methods

3.2.1 Sampling procedure and characterization

Figure 3 shows the location of Kabwe and the sampling points for the mining residue materials MRM and soil samples. The legacy mine has a sulfide ore body confined with secondary mineralization oxide zones of silicate ore such as willemite (Zn_2SiO_4), cerussite ($PbCO_3$), quartz (SiO_2), smithsonite ($ZnCO_3$), goethite (FeOOH), hematite (Fe_2O_3), and metal-bearing; vanadates, phosphates, carbonates of Zn, Pb, and V (Kamona

and Fredrick, 2007). The MRMs were randomly collected from the dumpsite in the form of agglomerated particles; hence, they were lightly crushed with an agate mortar and pestle, air-dried, and sieved using a combination of aperture screens, i.e., < 30 µm, 30-75 µm, 75-150 µm, 150-250 µm, 250-500 µm, and 2 mm stainless sieves.

The topsoil samples (5 cm deep) were collected within a 10 km radius of the dumpsite. The samples were sieved through < 30 µm and 2 mm. The < 30 µm particles were further characterized using laser diffraction (Microtrac® MT3300SX, Nikkiso Co. Ltd., Osaka) for particle size variability in the aerosols from the MRM and soil samples. Initially, particles < 62.5 µm are susceptible to wind dispersion (depending on particle classification) (Kok et al., 2012). In this study, inhalable dust was assessed from aerosals (< 30 µm). A comparison in the particle size distribution for the < 30 µm particles is shown in figure 11. Approximately 50% of particles have an effective diameter of 10 to 20 µm. Particles < 20 µm represent inhalable dust following an accident inhalation of contaminated soil or the MRM, which are likely to be deposited in the upper respiratory tract. Among the samples collected, the MRM has the highest volume of < 10 µm particles. Particles < 10 µm can easily reach the tracheobronchial of the human lungs (Guney et al., 2017).

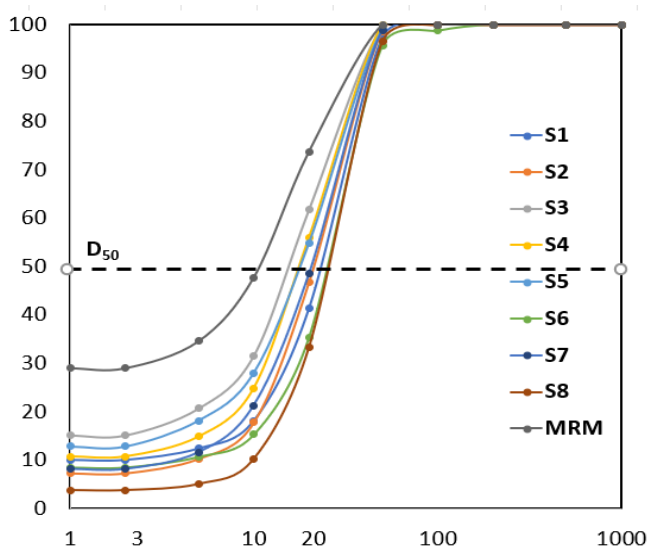

Figure 11. Particle size distribution in (< 30 µm) with their 50% effective diameter

The X-ray diffractometer (XRD) (MultiFlex, Rigaku Corporation, Tokyo, Japan) and X-ray fluorescence spectrometer (XRF) (SpectroXepos, Rigaku Corporation, Tokyo, Japan) were used on samples (< 50 µm in diameter) for mineralogy and chemical composition, respectively. The total content (bulk samples) from XRF was compared with the total content from aqua regia (AR) (HCl/HNO_3, 3:1 solution) (ISO 11466, 1995); the digestion was conducted on samples (< 2 mm) on the hot plate at 120 °C for 1 hr. The total organic carbon (TOC) content was obtained by the difference between the total carbon (TC) content and the inorganic carbon (IC) content, measured using a total carbon analyzer with a solid sample combustion unit (TOC-VCSH-SSM-5000A, Shimadzu Corporation, Kyoto, Japan).

3.2.2 Sequential extraction

The extraction procedure was based on the earlier works of Marumo et al. (2003) and Tessier et al. (1979). The method partitioned the target elements into five phases (1) exchangeable, (2) carbonates, (3) iron and manganese oxides, (4) organic matter and sulfide minerals, and (5) residual. One gram of solid sample for each particle size (< 30 µm, 30-75 µm, 75-150 µm, 150-250 µm, 250-500 µm) was used. The details of the extraction procedure are summarized below.

i. Phase 1 (Exchangeable): 1 g of soil sample was mixed with 20 ml of 1M $MgCl_2$ at pH 7, shaken at 200 rpm for 1 h at room temperature.

ii. Phase 2 (Bound to carbonates): The residual soil sample from Phase 1 was extracted with 20 ml of 1M CH_3COONa at pH 5 and shaken at 200 rpm for 5 h at room temperature.

iii. Phase 3 (Bound to Fe/Mn oxides): The residual soil sample from phase 2 was mixed with 20 ml of 0.04M $NH_2OH.HCl$ in 25% acetic acid, shaken at 120 rpm for 5 h at 80 °C.

iv. Phase 4 (Bound to organic matter and sulfide minerals): The residual from phase 3, mixed with the solution of 20 ml of 0.04M $NH_2OH.HCl$ in 25% acetic acid, 8 ml of 30% H_2O_2, and 8 ml of 0.02M HNO_3 shaken at 120 rpm for 5 h at 80 °C.

v. Phase 5 (Residual): 20 ml of 60% HNO_3 was used to extract residues from phase 4 at 120 °C for 1 h, then diluted in a 100 ml volumetric flask.

The leachates from the extraction procedures were analyzed using inductively coupled plasma mass spectrometry (ICP-MS) (ICAP Qc, Thermo Fisher Scientific, Waltham, MA, USA). All chemicals used for the experimental analysis were reagent grade (Wako Pure Chemical Industries Ltd. Osaka, Japan).

3.2.3 In-vitro solubility and bioaccessibility tests

We performed the solubility leaching tests in simulated fluid (ALF, GS and PBS) using Japanese standard leaching tests; JLT-46 Environment Agency Notification No.46, an environmental standard for wastes and soil, and JLT-18 MOEJ Notification No. 19, acid extraction for oral intake. The extraction procedure for oral ingestion of MRM and soil samples was done by mixing 3 g (< 2 mm) of solid samples with 100 ml of 1mol/L HC*l* followed by reciprocal shaking at 200 rpm for 2 h. The leachates were filtered through 0.45 µm Millex® syringe-driven sterile membrane filters and stored in air-tight containers. The concentrations of Pb and Zn were then analyzed by inductively coupled plasma atomic emission spectroscopy (ICP-AES). The (ALF, GS and PBS) were prepared according to Pelfrêne et al. (2017). The composition of the fluids is presented in Table 9. To assess the solubility of Pb and Zn from MRM and soil samples in the simulated fluids (ALF, PBS and GS), 3 g of particles (< 30 µm) were mixed with 30 ml of each solution for 6 h at 200 rpm. After the leaching experiments, the pH, temperature, oxidation-reduction potential (ORP) and suspension's electrical conductivity (EC) were measured. For accuracy and precision, all batches were performed in triplicates. The concentrations of Pb and Zn were then analyzed by inductively coupled plasma atomic emission spectroscopy (ICP-AES). The bioaccessible fractions of Pb and Zn via ingestion or inhalation were determined using the following formula.

$$\text{Bioaccessible fraction (BF)\%} = (C_{bio}/C_{\text{Total content}})*100$$

Where, C_{bio} is the concentration of the Pb and Zn in < 30 µm particles via inhalation (ALF, GS and PBS) or ingestion (HC*l*) and $C_{\text{Total content}}$ is the total content (AR digestion) of Pb and Zn in MRM or soil samples.

Table 9. Composition of simulated fluids; artificial lysosomal fluid (ALF), gamble solution (GS), and phosphate-buffered saline (PBS) (Pelfrêne et al., 2017)

Composition (g/L)	ALF	GS	PBS
NaCl	3.21	6.779	8.77
$Na2HPO_4$	0.071		1.28
$NaHCO_3$		2.268	
Trisodium citrate dihydrate	0.077	0.055	
NH4Cl		0.535	
Glycine	0.059	0.375	
NaH_2PO_4		1.872	
L-cysteine		0.121	
NaOH	6		
Citric acid	20.8		
$CaCl_2 \cdot 2H2O$	0.128	0.026	
Na_2SO_4	0.039		
$MgCl_2 \cdot 6H_2O$	0.05		
Disodium tartrate	0.09		
Sodium lactate	0.085		
Sodium pyruvate	0.172		
KH_2PO_4			1.36
DPPC 4 (surfactant)			
Properties			
pH	4.5 ± 0.1	7.3 ± 0.1	7.3 ± 0.1
Ionic strength (mol/L)	0.34	0.17	0.19

4. Results and discussion

4.2.1 Total content of the samples

Table 10 shows the contents of Pb and Zn by XRF and AR digestion of MRM and topsoils. The total content of Pb and Zn in MRM with XRF was more profound than pseudo-total content from AR digestion. From the assessment of the two methods, it can be demonstrated that the contents for both elements in MRM range from 16,000 to 71,000 mg/kg. The contents of Pb and Zn showed a good correlation in the soil samples, although acid digestion was more than XRF results in some samples. The contents of Pb and Zn in the soils ranged from 102 to 3,320 mg/kg. The contents in the soil were higher than the permissible limit set by The World Health Organization (WHO) of 85 and 50 mg/kg for Pb and Zn, respectively. This can be attributed to the deposition of fine particles from the mine area (Nakamura et al., 2021). The authors (Kribek et al., 2019, Mufalo et al., 2021, Nakamura et al., 2021, Tembo et al., 2006) highlighted that anthropogenic contamination

in the surrounding soil was dependent on the distance from the mine wastes and the direction of prevailing winds. The higher contents from both assessment methods suggest the predominance of airborne contamination from the legacy mine (Ether et al., 2005, Mufalo et al., 2021, Tangvroon et al., 2020).

Table 10. Total contents of mininig residue material (MRM) and soil samples from XRF and Aqua regia (AR)

Sample	Aqua regia Pb (mg/kg)	XRF Pb (mg/kg)	Aqua regia Zn (mg/kg)	XRF Zn (mg/kg)	TOC (wt.%)
MRM	59,000	71,000	16,000	23,000	0.4
S1	3,210	3,320	1,990	2,600	2.5
S2	710	1,080	853	1,990	1.9
S3	1,190	1,070	693	750	2.8
S4	200	265	180	359	0.5
S5	357	633	279	399	0.5
S6	699	863	1,110	1,370	0.8
S7	1,710	1,770	1,300	1,840	1.5
S8	1900	3,170	1,320	2,090	5

4.2.2 Solubility and bioaccessibility Pb and Zn in HC*l*, ALF, PBS, and GS

Table 11 shows the solubility of Pb and Zn in HC*l* and the simulated fluids in the MRM and soil samples S1 to S8. The solubility of Pb and Zn was higher with HC*l* when compared with solubility in ALF, PBS, and GS fluids. The bioaccessible Pb in MRM was 13 times higher compared to ALF and no Pb was soluble with PBS and GS; however, Zn was observed with PBS and GS, corresponding to bioaccessible fractions of 7.4 and 0.9%, respectively. The bioaccessible fractions for Pb with ALF in the soil samples ranged from 7 to 37%. The bioaccessible fractions were lower compared to those of HC*l* (56 to 86%). The results suggest that oral ingestion of contaminated soil could be the primary exposure route for the uptake of toxic elements into the bloodstream. Table 12 illustrates the changes in pH, EC, and ORP after leaching with the simulated fluids. The MRM's pH did not relatively change after leaching with all the three simulated fluids (around 4 - 5.9). However, only Zn was observed to leach out from the MRM. This could be attributed to the high solubility of Zn (Metwally et al., 1993, Mignardi et al., 2012). The presence of organic compounds represented by proteins, glycine, cysteine and carbonates in GS and

PBS may favor the chemical formation of insoluble complexes at neutral pH (Khelifi et al.,2021). This could be the reason why no Pb was observed in the soil samples after leaching with GS and PBS. However, with ALF, the pH in all the soil samples significantly changed from the overall neutral pH range of (6.2 – 8.2) to around (4 to 4.8). Higher metal release rates are expected in ALF than in GS solution or PBS since ALF is a more aggressive solution (lower pH). Liu et al. (2021) also observed higher bioaccessible fractions of toxic elements in ALF than in GS. Guney et al. (2017) extracted higher bioaccessible fractions of Pb and Zn in < 20 µm (representing the tracheobronchial region) with ALF than GS, which is consistent with our results. The pH critically plays a vital role in the bioaccessibility of toxic elements. Although ALF was much more aggressive than GS and PBS, metal solubility is higher with HC*l* because in the stomach environment, the pH usually fluctuates around pH of 1.5 to 3. Sold/liquid ratios and particle size may also influence the solubility of toxic elements in simulated fluids (Pelfrêne et al., 2017).

Table 11. Solubility (mg/kg) and bioaccessible fractions (BF) of Pb and Zn from mining residual material (MRM) and soil samples (S1 to S8) in simulated fluids and hydrochloric acid (HC*l*)

Element	Solution/sample	MRM	S1	S2	S3	S4	S5	S6	S7	S8
Pb (mg/kg)	Bulk HC*l* (< 2 µm)	22,800	2,660	533	1,160	133	200	500	1,530	1,630
	BF%	39	83	75	79	67	56	72	89	86
Pb (mg/kg)	ALF (< 30 µm)	1,700	871	122	226	42	102	51	462	709
	BF%	2.9	27.1	17.1	19	21	28.6	7.3	27	37.3
Zn (mg/kg)	Bulk HC*l* (< 2 µm)	11,700	1,190	307	530	63	62	797	717	883
	BF%	73	60	36	76	35	22	72	55	67
Zn (mg/kg)	ALF (< 30 µm)	6,470	646	147	59	26	53	99	545	617
	BF%	40.4	32.5	17.2	8.5	14.4	19	8.9	41.9	46.7
Zn (mg/kg)	PBS (< 30 µm)	1,190	-	-	-	-	-	-	-	-
	BF%	7.4	-	-	-	-	-	-	-	-
Zn (mg/kg)	GS (< 30 µm)	142	-	-	-	-	-	-	-	-
	BF%	0.9	-	-	-	-	-	-	-	-

Table 12. The changes in pH, EC, and ORP before and after extraction with simulated fluids (ALF, PBS, and GS)

Sample		MRM	S1	S2	S3	S4	S5	S6	S7	S8
Before	pH	5.2	6.3	7.1	7.5	6.2	8.2	8.2	7.7	7.1
	EC (mS/m)	2.8	0.13	0.06	0.08	0.04	0.19	0.25	0.23	0.57
	ORP (mV)	351	214	177	158	199	142	152	161	193
After (ALF- 4.5)	pH	4.02	4.43	4.45	4.53	4.5	4.62	4.78	4.55	4.02
	EC (mS/m)	16.7	14.6	13.4	14.7	14.6	14.9	15.1	14.6	16.7
	ORP (mV)	616	547	546	515	540	549	536	581	616
After (PBS-7.3)	pH	4.9	6.7	6.9	7.2	7	7.4	7.3	7.2	7.3
	EC (mS/m)	17.7	14.8	14.1	15.	14.5	14.1	15.4	14.9	14.9
	ORP (mV)	482	482	491	461	464	470	455	459	459
After (GS-7.3)	pH	5.9	7.05	7.08	7.23	7.2	7.4	7.41	7.3	7.2
	EC (mV)	16.9	13.6	12.3	13.7	14.2	14.1	14.2	13.9	13.5
	ORP (mV)	432	103	89	80	73	72	75	92	100

4.2.3 Solid-phase partitioning of Pb and Zn in MRM and soil samples

Figure 12 illustrates the sequential extraction of MRM in various particle sizes (< 30 µm, 30-75 µm, 75-150 µm, 150-250 µm, 250-500 µm) for Pb (a) and Zn (b). There were no distinct differences in Pb and Zn partitioning for different particle sizes. Generally, it is expected to have higher fractions in smaller particles; however, we could not observe any significant differences among the various particle sizes. This could be attributed to the milling process during the historic mining; over time, the particles could have aggregated and disintegrated to their actual size during leaching, hence the similar partitioning fractions. In contrast, Pb concentration increases with decreased particle size in smelter derived wastes. For example, Ettler et al. (2020) found higher contents and bioaccesibility of Pb and Zn in < 10 and < 48 µm slag samples of Kabwe than in the bulk samples. The results were comparable to Xu and Fu. (2022) who observed a similar trend in slag samples, however, the latter found that metal bioaccessibility in some finer particles was not significantly higher than in coarser particles. The similar Pb fractions, independent of size fractions suggests the decreased Pb bioavailability in MRM, relative to smelter-derived wastes, for a given particle size. Moreover, most of the Pb in the various particle sizes of MRM were in the sulfide/organic phase (17 to 23%) and residues (49- 53%). This means that the Pb was relatively stable after dumping at the mine site. For Zn, higher fractions of 15 to 22% were observed in the exchangeable fraction compared to Pb (9 to 12%). This explains the high solubility of Zn in the simulated fluids; freer Zn^{+} ions were readily available for exchange with the environment. However, at

least 33 and 51% of Pb and Zn respectively, absorbed to exchangeable, carbonates, Fe/Mn oxides could dissolve from the MRM when subjected to strong acidic conditions. The extracted phases in MRM by HC*l* were similar to extractable phases in the soil samples. Figure 12 illustrates the comparison between HC*l* extraction and sequential extraction (exchangeable + carbonates +Fe/Mn oxides phases) on the soil samples. The results showed a good correlation $r = 0.98$ and $r = 0.94$ for Pb and Zn, respectively. This suggests that HC*l* digestion could dissolve the exchangeable, carbonates and Fe/Mn oxides phases in the soil. Therefore, in an extreme case of fasting conditions a substantial amount of the toxic elements could be released into the stomach if contaminated soil were accidentally ingested.

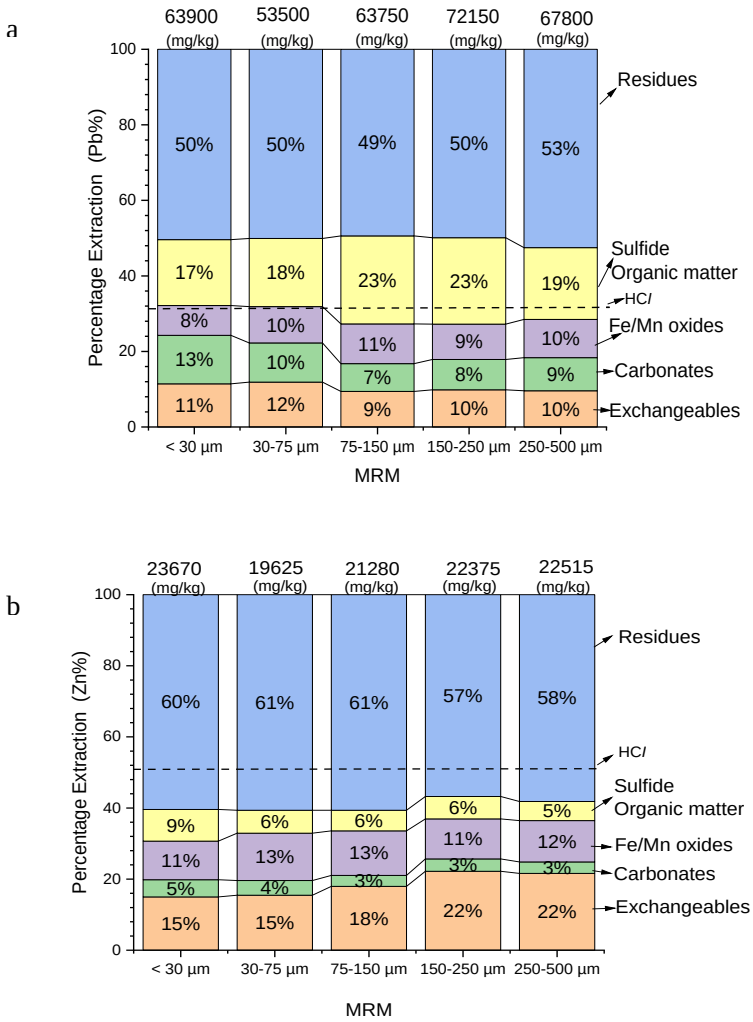

Figure 12. Solid-phase partitioning of Pb and Zn in various particle sizes in mining residual material (MRM)

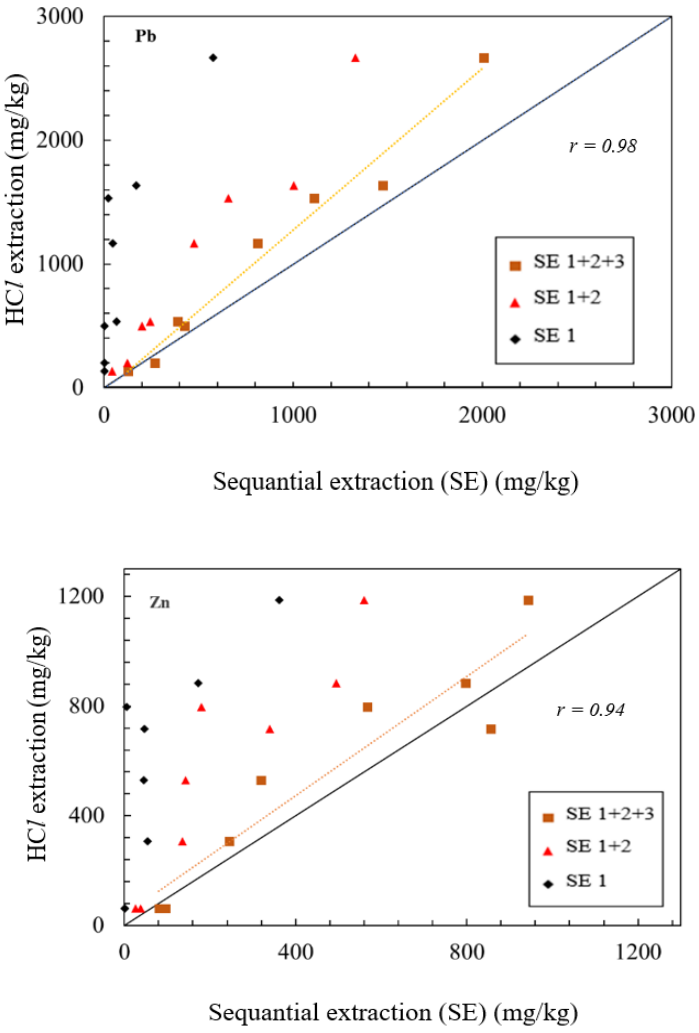

Figure 13. Comparison between HC*l* extraction and sequential extraction (SE 1: exchangeable, SE1+2: exchangeable+carbonates, SE 1+2+3: exchangeable+carbonates+ Fe/Mn oxides.

5. Conclusion

This paper discussed the efficacy of simulated fluids and HC*l* in the dissolution of Pb and Zn from MRM and soil samples near the Kabwe mine area. The higher solubility of Pb and Zn was observed with HC*l* extraction compared to the simulated fluids. The HC*l* aggressively dissolves the exchangeable, carbonates and Fe/Mn oxides. Comparing exposure routes, i.e., inhalation and ingestion for the uptake of Pb from contaminated soil or mine wastes, ingestion is more significant. The high Pb blood levels found in the residents of Kabwe can be related to ingestion of contaminated soil or dust containing high levels of Pb. Substantial amounts of Pb could be released in the stomach

(low pH), resulting in high adsorption of the toxic element into the bloodstream. Children are likely to be more affected than adults because of their hand-to-mouth activities. Furthermore, regardless of particle size, the solid-phase partitioning of MRM did not change significantly. However, at least 33% of Pb in the (exchangeables, carbonates, and Fe/Mn oxides) are mobilizable under acidic conditions.

References

Abraham, J., Dowling, K. and Florentine, S., 2018. Assessment of potentially toxic metal contamination in the soils of a legacy mine site in Central Victoria, Australia. Chemosphere, 192, pp. 122-132.

Baieta, R., Mihaljevič, M., Ettler, V., Vaněk, A., Penížek, V., Trubač, J., Kříbek, B., Ježek, J., Svoboda, M., Sracek, O. and Nyambe, I., 2021. Depicting the historical pollution in a Pb–Zn mining/smelting site in Kabwe (Zambia) using tree rings. Journal of African Earth Sciences, 181, 104246.

Bose-O'Reilly, S., Yabe, J., Makumba, J., Schutzmeier, P., Ericson, B. and Caravanos, J., 2018. Lead intoxicated children in Kabwe, Zambia. Environmental Research, 165, pp. 420-424.

Ettler, V., Vaněk, A., Mihaljevič, M. and Bezdička, P., 2005. Contrasting lead speciation in forest and tilled soils heavily polluted by lead metallurgy. Chemosphere, 58(10), pp. 1449-1459.

Guney, M., Bourges, C.M.J., Chapuis, R.P. and Zagury, G.J., 2017. Lung bioaccessibility of As, Cu, Fe, Mn, Ni, Pb, and Zn in fine fraction (< 20 μm) from contaminated soils and mine tailings. Science of the Total Environment, 579, pp.378-386.

Helser, J. and Cappuyns, V., 2021. Trace elements leaching from pbzn mine waste (plombières, belgium) and environmental implications. Journal of Geochemical Exploration, 220, 106659.

Kamona, A.F. and Friedrich, G.H., 2007. Geology, mineralogy and stable isotope geochemistry of the Kabwe carbonate-hosted Pb–Zn deposit, Central Zambia. Ore Geology Reviews, 30(3-4), pp. 217-243.

Khelifi, F., Caporale, A.G., Hamed, Y. and Adamo, P., 2021. Bioaccessibility of potentially toxic metals in soil, sediments and tailings from a north Africa phosphate-mining area: Insight into human health risk assessment. Journal of Environmental Management, 279, 111634.

Kok, J.F., Parteli, E.J., Michaels, T.I. and Karam, D.B., 2012. The physics of wind-blown sand and dust. Reports on Progress in Physics, 75(10), 106901.

Kříbek, B., Nyambe, I., Majer, V., Knésl, I., Mihaljevič, M., Ettler, V., Vaněk, A., Penížek, V. and Sracek, O., 2019. Soil contamination near the Kabwe Pb-Zn smelter in Zambia: Environmental impacts and remediation measures proposal. Journal of Geochemical Exploration, 197, 159-173.

Li, X., Gao, Y., Zhang, M., Zhang, Y., Zhou, M., Peng, L., He, A., Zhang, X., Yan, X., Wang, Y. and Yu, H., 2020. In vitro lung and gastrointestinal bioaccessibility of potentially toxic metals in Pb-contaminated alkaline urban soil: The role of particle size fractions. Ecotoxicology and Environmental Safety, 190, 110151.

Liu, J., Zhang, A., Chen, Y., Zhou, X., Zhou, A. and Cao, H., 2021. Bioaccessibility, source impact and probabilistic health risk of the toxic metals in PM2. 5 based on lung fluids test and Monte Carlo simulations. Journal of Cleaner Production, 283, 124667.

Marumo, K., Ebashi, T. and Ujiie, T., 2003. Heavy metal concentrations, leachabilities, and lead isotope ratios of Japanese soils. Shigen-Chihsitsu. 53,pp. 125–146.

Metwally, A.I., Mashhady, A.S., Falatah, A.M. and Reda, M., 1993. Effect of pH on zinc adsorption and solubility in suspensions of different clays and soils. Zeitschrift für Pflanzenernährung und Bodenkunde, 156(2), pp. 131-135.

Mignardi, S., Corami, A. and Ferrini, V., 2012. Evaluation of the effectiveness of phosphate treatment for the remediation of mine waste soils contaminated with Cd, Cu, Pb, and Zn. Chemosphere, 86(4), pp. 354-360.

Mufalo, W., Tangviroon, P., Igarashi, T., Ito, M., Sato, T., Chirwa, M., Nyambe, I., Nakata, H., Nakayama, S. and Ishizuka, M., 2021. Solid-Phase partitioning and leaching behavior of Pb and Zn from playground soils in Kabwe, Zambia. Toxics, 9(10), 248.

Nakamura, S., Igarashi, T., Uchida, Y., Ito, M., Hirose, K., Sato, T., Mufalo, W., Chirwa, M., Nyambe, I., Nakata, H., Nakayama, S. and Ishizuka M., 2021. Evaluation of

dispersion of Lead-Bearing Mine Wastes in Kabwe District, Zambia. Minerals, 11(8), 901.

Pelfrêne, A., Cave, M.R., Wragg, J. and Douay, F., 2017. In vitro investigations of human bioaccessibility from reference materials using simulated lung fluids. International Journal of Environmental Research and Public Health, 14(2), 112.

Reyes, A., Cuevas, J., Fuentes, B., Fernandez, E., Arce, W., Guerrero, M. and Letelier, M.V., 2021. Distribution of potentially toxic elements in soils surrounding abandoned mining waste located in Taltal, Northern Chile. Journal of Geochemical Exploration, 220, 106653.

Soltani, N., Keshavarzi, B., Moore, F., Cave, M., Sorooshian, A., Mahmoudi, M.R., Ahmadi, M.R. and Golshani, R., 2021. In vitro bioaccessibility, phase partitioning, and health risk of potentially toxic elements in dust of an iron mining and industrial complex. Ecotoxicology and Environmental Safety, 212, 111972.

Tabelin, C.B., Igarashi, T., Villacorte-Tabelin, M., Park, I., Opiso, E.M., Ito, M. and Hiroyoshi, N., 2018. Arsenic, selenium, boron, lead, cadmium, copper, and zinc in naturally contaminated rocks: A review of their sources, modes of enrichment, mechanisms of release, and mitigation strategies. Science of the Total Environment, 645, pp. 1522-1553.

Tangviroon, P., Noto, K., Igarashi, T., Kawashima, T., Ito, M., Sato, T., Mufalo, W., Chirwa, M., Nyambe, I., Nakata, H, Nakayama, S, and Ishizuka, M., 2020. Immobilization of lead and zinc leached from mining residual materials in Kabwe, Zambia: Possibility of chemical immobilization by dolomite, calcined dolomite, and magnesium oxide. Minerals. 10(9), 763.

Tembo, B.D., Sichilongo, K. and Cernak, J., 2006. Distribution of copper, lead, cadmium and zinc concentrations in soils around Kabwe town in Zambia. Chemosphere, 63(3), pp. 497-501.

Tessier, A., Campbell, G.C. and Bisson, M., 1979. Sequential extraction procedure for the speciation of particulate trace metals. Anal. Chem. 51,pp. 844–851

Weggeberg, H., Benden, T.F., Steinnes, E. and Flaten, T.P., 2019. Element analysis and bioaccessibility assessment of ultrafine airborne particulate matter (PM0. 1) using simulated lung fluid extraction (artificial lysosomal fluid and Gamble's solution). Environmental Chemistry and Ecotoxicology, 1, pp. 26-35.

Xu, D.M. and Fu, R.B., 2022. The mechanistic understanding of potential bioaccessibility of toxic heavy metals in the indigenous zinc smelting slags with multidisciplinary characterization. Journal of Hazardous Materials, 425, 127864.

Chapter 4

THE PERFORMANCE OF HALF-BURNT DOLOMITE IN COLUMN EXPERIMENTS AND VALIDATION IN PILOT EXPERIMENTS

4 Introduction

The historical Pb-Zn mine in Kabwe, Zambia, has significantly impacted the small town's environment. Over a decade since the mine closure has passed, contamination from the mine wastes remains challenging. Laboratory scale experiment proposals and countermeasures using biochar, phosphate, and half-burnt dolomite have shown potential in attenuating the toxic elements lead (Pb) and zinc (Zn). However, the methods do not represent the actual flow conditions in the environment. Tabelin et al. (2012) highlighted that the solid to liquid variations, competition between H^+ and the dissolved metals for ligands (e.g., OH^-, CO_3^{2-}, SO_4^{2-}, S^{2-} and phosphates), temperature, and pore water flow rates affect the toxic heavy metal release and retention. Reasonable prediction and validation in the attenuation of toxic elements could be possible in actual field conditions such as implementing ex situ remediation. In situ and ex situ remediation are two techniques for heavy metal contaminated sites. The in situ method is more cost-effective than the ex-situ, while the latter has a higher efficiency in heavy metal remediation. Many ex-situ remediation costs come from excavation and transportation of the contaminated materials from the polluted area. The in situ technique, on the other hand, can be performed on-site. For this reason, many researchers have been working on discovering new methods and improving the efficiency of the in situ technique (Ali et al., 2017; Andrunik et al., 2020; Bolan et al., 2014; Farrell and Jones., 2010; He et al., 2013; Kumpiene et al., 2008; Mahar et al., 2015; Seshadri et al., 2017; Tangviroon et al., 2017; Tangviroon and Igarashi, 2017). However, actualizing such technology requires a cheap and efficient immobilizer for the contaminated site. The author's previous research investigated a cheap and abundant immobilizer i.e., half-burnt dolomite (HBD) to remediate Pb and Zn leached from mining residue materials (MRM).

The HBD was a modified product of the abundant local material (dolomite). Dolomite ($CaMg(CO_3)_2$) is formed when the limestone or carbonate mud is modified by replacing limestone's calcium ions with magnesium-rich ions (Pehlivan et al., 2009).

Dolomite calcination produces a new immobilizer containing magnesia (MgO) and calcite ($CaCO_3$). However, in our previous research, the analyses were done based on the batch leaching, where the HBD was added to the MRM in a predetermined volume of water and then shaken for a set period, thus allowing us to assess the immobilization potential of the HBD. In other words, the batch leaching experiments did not seem to be a reasonable prediction of the actual transport of contaminants due to several reasons, such as different solid-to-liquid ratios and flow paths of water from those in the field (Tabelin et al., 2010, 2014). An in-depth understanding of the Pb and Zn immobilization from MRM and HBD mixtures is still needed because the bioavailability of metals may vary due to environmental conditions (Vrînceanu et al., 2019). Therefore, column experiments could provide necessary conditions for mimicking the flow conditions in the environment. To actualize the attenuation mechanism of HBD in column experiments, we compared the results with those of pilot experiments in the actual field by excavating the MRM from Kabwe, followed by the addition of HBD.

Therefore, this research aims to investigate the long-term potency of HBD in MRM and the mechanism of immobilization over several weeks in column experiments and compare the leaching of Pb and Zn in pilot experiments representing the actual field conditions. The current study will assist in developing chemical immobilization for remediating heavy metal contaminated sites in Zambia.

4.1 Materials and Methods

4.2.1 Sample collection and excavation

The sampling of MRM was conducted at the dumping site of Pb-Zn mine waste located in Kabwe, Zambia. The MRM was randomly collected using shovels, brought to the laboratory, dried under ambient conditions, crushed, sieved through a 2-mm aperture screen, and kept in air-tight containers before usage. Construction of the embankments for the pilot experiments was done at the University of Zambia (UNZA), located about 120 km from the dumping site. The MRM was excavated from Kabwe and brought to UNZA to four embankments.

4.2.2 Column Experiments

Figure 14 shows the schematic illustration of the columns. The columns and rainfall simulators were transparent polyvinyl chloride (PVC) tubes. The inner diameter of the column was 5.2 cm, and its height was 60 cm. They were vertically mounted on a steel stand and covered with rainfall simulators. These covers are designed with small holes to simulate the raindrops and protect the sample inside the column from dust contamination. The experimental setup in the columns included pure MRM (HBD_0) and MRM mixed with 1%, 5%, and 10% of HBD, denoted as HBD_1, HBD_5, and HBD_{10}, respectively. The sample packaging in the columns was homogenized by compacting 49 g of samples to a thickness of 2 cm until 10 cm for each column. At the bottom of each column, a filter paper was placed on the top of the polytetrafluoroethylene net (PTFE) on a PVC plate with holes to prevent the leaking of the solid particles. All the column experiments were carried out under ambient conditions to mimic the dumping environment.

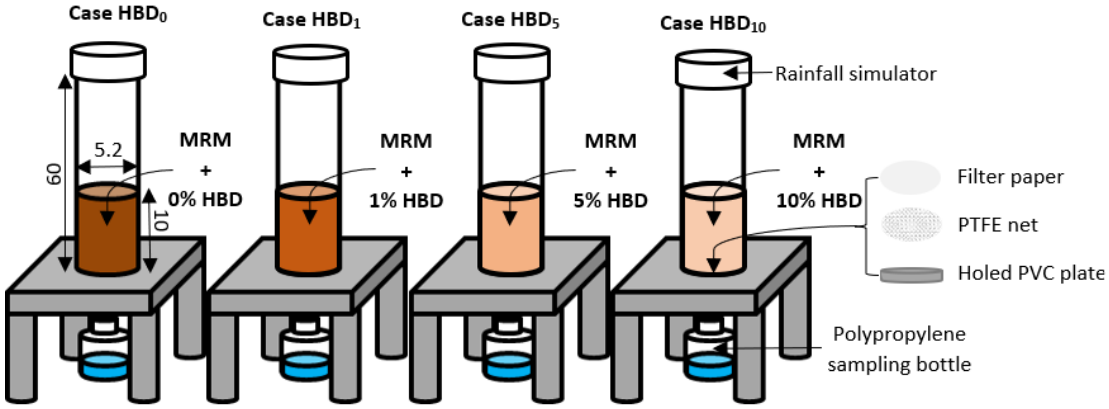

Figure 14. Schematic diagrams of the columns (all units are in cm)

4.2.3 Irrigation and collection of effluents

Every week, 100 ml of deionized water was irrigated all at once via the rainfall simulator and gravitationally percolated through the packed samples. The amount of irrigation is equivalent to the average rainfall during the wet season (October to March) in Kabwe, Zambia. Polypropylene bottles were used to collect the effluent at the lower end of each column. The effluent was collected every week, followed by pH, electrical conductivity (EC), and oxidation-reduction potential (ORP) measurements before the

next irrigation. The effluents were filtered through 0.45-µm Millex® filters and stored in air-tight polypropylene bottles before chemical analysis.

4.2.4 post-experimental analysis

After the termination of the experiments, all columns were disassembled. The solid residuals were then air-dried and separately kept in polypropylene bottles prior to the sequential extraction experiments. The sequential extraction experiments were performed to compare the variability of solid-phase (Pb and Zn) speciation in the columns after the experiments. The procedure is described in section 4.2.6.

4.2.5 Design of embankments

Figure 15 shows the design of the embankments. The design of the embankments included the use of wooden boards supported by 300 mm of soil to hold the MRM and an impervious layer to prevent the leaching of hazardous metals into the groundwater. Meanwhile, dolomite was collected from a local quarry company, sieved through aperture screens of < 2 mm. After sieving, the HBD was produced by burning dolomite in a furnace at 700˚C for 2 h and stored in air-tight containers. The efficacy of HBD was assessed by four case studies using 10% ratio of HBD with MRM in the embankments (case 1 and 2) (Table 13). At the bottom of each embankment a combination of surface soil and 10 % HBD was used as the base for the MRM.

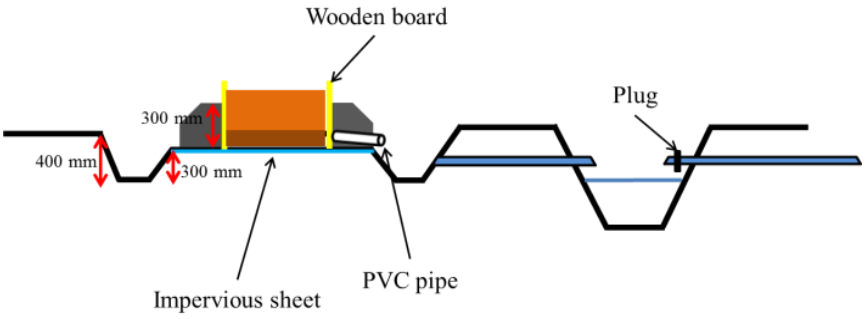

Figure 15. Schematic representation of the embarkments

Table 13. Conditions of the pilot-scale experiments

	Case 1	Case 2	Case 3	Case 4
①		Surface Soil from UNZA	Surface Soil from UNZA	Surface Soil from UNZA+Plants
②	Mine waste+ 10% half-burnt dolomite	Mine waste+ 10% half-burnt dolomite	Mine waste	Mine waste
③	Surface Soil from UNZA+ 10% half-burnt dolomite	Surface Soil from UNZA+ 10% half-burnt dolomite	Surface Soil from UNZA+ 10% half-burnt dolomite	Surface Soil from UNZA+ 10% half-burnt dolomite

4.2.6 Sample characterization

The fresh MRM were examined by scanning electron microscopy with energy-dispersive X-ray spectroscopy (SEM-EDS, InTouchScope™, JSM-IT200, JEOL Ltd., Japan). Pressed samples of finely crushed powder (< 50 μm in diameter) of the MRM and HBD were prepared for chemical and mineralogical analyses by an X-ray fluorescence spectrometer (XRF) (SpectroXepos, Rigaku Corporation, Tokyo, Japan) and X-ray diffractometer (XRD) (MultiFlex, Rigaku Corporation, Tokyo, Japan). The organic carbon (OC) content was obtained by subtracting the total carbon (TC) content from the inorganic carbon (IC) content. The TC and IC were analyzed using a total carbon analyzer with a solid sample combustion unit (TOC-VCSH-SSM-5000A, Shimadzu Corporation, Kyoto, Japan).

Sequential extraction was conducted to determine the solid-phase speciation of Pb-Zn in the MRM. The procedure used in this study was taken from Marumo et al. (2003). The improved procedure is based on two well-known techniques, Tessier et al. (1979) and Clevenger. (1990), which have been used extensively to characterize tailings, mineral processing wastes, and leaching residuals (Anju and Banerjee., 2010; Dang et al., 2002; Khoeurn et al., 2018). It fractionates heavy metals into five phases: exchangeable, carbonates, Fe-Mn oxides, sulfide/organic matter, and residual. Details of the sequential extraction procedure are illustrated in Table 14. The experiments were conducted on 1 g of less than 2 mm diameter samples. After each extraction step, the centrifugation of the suspension was done at 3,000 rpm for 30 min to retrieve the extractant. The residual was washed with 20 ml of deionized water, followed by centrifugation to separate the residual from the washing solution, and brought to the next extraction step. The extractant and

washing solution were combined and diluted to 50 ml for steps 1 to 4 and 100 ml for step 5, filtrated through 0.45-μm Millex® filters (Merck Millipore, Burlington, MA, USA), and kept in polypropylene bottles before analysis. Note that our previous studies have proved this extraction procedure to be reproducible with an average precision of 7% (Huyen et al., 2019; Vongphuthone et al., 2017)

Table 14. Sequential extraction for heavy metals speciation

Phase	Extractant	L/S ratio (mL/g)	Temperature (°C)	Duration (h)	Speed (rpm)	Extracted phase
1	1 M $MgCl_2$ at pH 7	20/1	25	1	200	Exchangeable
2	1 M CH_3COONa at pH 5	20/1	25	5	200	Carbonates
3	0.04 M $NH_2OH{\cdot}HCl$ in 25% acetic acid at pH 5	20/1	80	5	120	Reducible
4	0.04 M $NH_2OH{\cdot}HCl$ in 25% acetic acid; 30% H_2O_2; 0.02 M HNO_3	36/1	80	5	120	Oxidizable
5	60% HNO_3	20/1	120	1		Residue

4.2.7 Chemical analysis of the liquid sample

Concentrations of Pb, Zn, and coexisting ions were quantified by an inductively coupled plasma atomic emission spectrometer (ICP-AES) (ICPE-9000, Shimadzu Corporation, Kyoto, Japan) (margin of error = ± 2~3%, determination limit 0.01-0.001 mg/L). The analyses were done on pretreated samples, which were prepared by adding 1% by volume of 60% reagent-grade nitric acid (HNO_3) to the filtrated samples. The pretreatment was performed to ensure the complete dissolution of the target elements. The non-acidified samples were used for alkalinity determination, in which a known volume of sample was titrated with 0.01 M reagent-grade sulfuric acid (H_2SO_4) until pH 4.8. All chemicals used were reagent grade (Wako Pure Chemical Industries Ltd., Osaka, Japan).

4.2.8 Geochemical Modeling

Aqueous geochemical conditions of the effluents were determined using PHREEQC (Version 3, U.S. Geological Survey, Sunrise Valley Drive Reston, VA, USA). Thermodynamic properties of all calculations were taken from the MINTEQ database (Parkhurst and Appelo., 1999).

4.3. Results and discussion

4.3.1 Properties of MRM and HBD

The chemical and mineralogical compositions for MRM and immobilizer (HBD) are illustrated in Tables 15 and 16, respectively. The content of Fe_2O_3 (41.1%) was the highest among all chemical components detected. The Pb (7.1%) and Zn (2.3%) contents were lower than what was previously recorded (10.9% for Pb and 8.1% for Zn). The mineralogy of the MRM was like the previous study comprising anglesite ($PbSO_4$), followed by zinkosite ($ZnSO_4$), quartz (SiO_2), and minor amounts of goethite (FeOOH), hematite (Fe_2O_3), and gypsum ($CaSO_4 \cdot 2H_2O$). Although sulfide minerals were not detected in the MRM, SEM-EDS analysis of fresh MRM suggests the presence of sulfide minerals, oxidation of these minerals might be the source of Pb and Zn (Figure 16). The presence of anglesite and zinkosite indicates sulfide minerals' existence since the two minerals are well-known to be the common exchangeable products of Pb- and Zn-sulfides (Hayes et al. 2009). The HBD had similar chemical and mineralogical compositions reported in the author's previous study, amounting to Ca (62.4%) and Mg (33.3%), in the forms of dolomite ($CaMg(CO_3)_2$), calcite ($CaCO_3$), and magnesia (MgO). Many studies have reported that the three chemical components can immobilize heavy metals, including Pb and Zn (Trakal et al., 2011; Vrînceanu et al., 2019).

Table 15. Chemical composition of solid samples (the unit is in wt.%)

	MRM	HBD
SiO_2	21.4	0.37
TiO_2	0.3	<0.01
Al_2O_3	1.91	0.11
Fe_2O_3	41.1	0.68
MnO	1.4	0.43
MgO	<0.01	33.3
CaO	6.7	62.4
Na_2O	<0.01	<0.01
K_2O	<0.01	0.16
P_2O_5	<0.01	<0.01
SO_3	16.2	0.2
Pb	7.1	<0.01
Zn	2.3	<0.01
OC	<0.01	<0.01

Table 16. Mineralogical composition of solid samples

	MRM	HBD
Quartz	++	-
Gypsum	+	-
Anglesite	+++	-
Zinkosite	++	-
Hematite	+	-
Goethite	+	-
Dolomite	-	+++
Calcite	-	+
Magnesia	-	+

+++: strong、++: moderate、+: weak、-: none

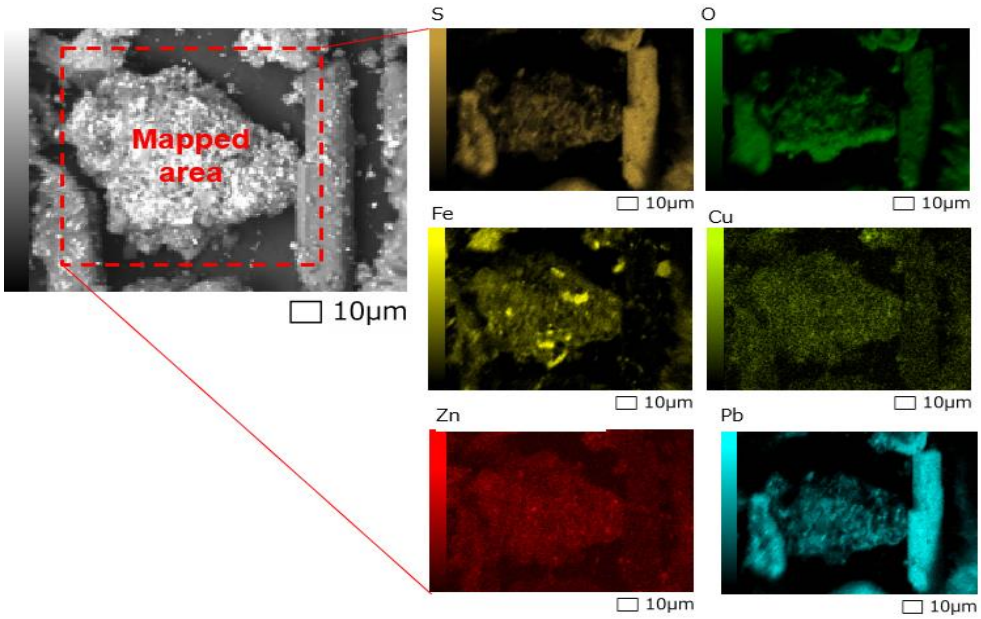

Figure 16. SEM photomicrograph of a representative sulfide mineral in mining residue maerials (MRM) and the corresponding elemental maps of Fe, S, O, Cu, Pb and Zn

4.3.2 Effect of HBD on leachate pH and major coexisting ions

Figure 17a illustrates the changes in the effluent pH throughout 30 weeks in the columns. The pH increased with increasing HBD addition (0 to 10%). Initially, the pH was low for MRM (HBD_0), then slightly increased after adding 1% (HBD_1), stabilizing at around 7.25. The pH values in the columns with 5% (HBD_5) and 10% (HBD_{10}) fluctuated within a narrow range of about 7.75 and 8, respectively. The results manifest the improvement of alkaline effluent properties due to HBD liming effect. The addition of HBD controls the pH by the equilibrium dissolution of dolomite (Equation 1), calcite (Equation 2), and magnesia (Equation 3) (Fu et al., 2018; Liu et al., 2018; Liu and Dreybrodt, 1997; Pokrovsky and Schott, 2001; Xing et al., 2018).

$$CaMg(CO_3)_2 + 2\,H^+ \;<=>\; Ca^{2+} + Mg^{2+} + 2HCO_3^- \qquad (1)$$

$$CaCO_3 + H^+ <=> Ca^{2+} + HCO_3^- \qquad (2)$$

$$MgO + H_2O <=> Mg(OH)_2 <=> Mg^{2+} + 2OH^- \qquad (3)$$

However, the lower pH in columns HBD_0 and HBD_1 could be attributed to not enough carbonate mineral dissolution to consume H^+ generated by oxidation of sulfide minerals. Generally, under atmospheric conditions with pH ranging from slightly acidic to

moderately alkaline, ferrous (Fe^{2+}) produced from sulfide mineral oxidation is oxidized to ferric (Fe^{3+}) and Fe^{3+} precipitates as Fe oxyhydroxide/oxide, which produces H^+ as a by-product (Chandra and Gerson, 2010; Lindsay et al., 2015). The addition of HBD yields divalent cations and generates carbonate species.

Figures 17(b-d) illustrate the leaching behaviors of Mg^{2+}, SO_4^{2-}, and Ca^{2+}. In all the columns, the leaching concentrations of Mg^{2+} and SO_4^{2-} were high at first and dramatically decreased before becoming steady. The behavior of these ions was observed in two distinct regions. The first one is characterized by high leaching and sharp reduction of Mg^{2+} and SO_4^{2-} concentrations, which lasted for 11 weeks. The trend reflects rapid releases of SO_4^{2-} and Mg^{2+}, indicating dissolutions of soluble secondary phase minerals, such as Fe sulfates and Mg sulfates (typical ubiquitous assemblages in acid mine drainage (AMD) affected systems) (Nordstrom and Alpers, 1999; Valente et al., 2016). The second one was a consistent trend from week 12 until the end of the experiments.

The leaching concentration of Ca^{2+} was disorderly, and no distinct trend could be observed in all the columns. The trend could be attributed to the inhibition of dolomite and calcite dissolution or the solubility of Ca-contained mineral(s). Phreeqc simulation on the saturation indices (*SIs*) showed that all effluents were under equilibrium conditions to gypsum ($CaSO_4 \cdot 2H_2O$) but were undersaturated with respect to $Mg(OH)_2$ (Figure 18). The solubility of gypsum restricted the leaching of Ca^{2+}, and thus, calcite and dolomite played an essential role in controlling effluent pH. Although the *SIs* of dolomite and calcite were less than the lower boundary of a standard error interval used to indicate saturation equilibrium (-0.2) in HBD_1, the dissolution of dolomite and calcite helped to increase leachate's pH in addition to the dissolution of magnesia. While the *SIs* of dolomite and calcite were higher than -0.2 throughout the experimental period in the case of HBD_{10}, and HBD_5, only calcite behaved similarly. The saturation index of dolomite in HBD_5 was over -0.2 at the beginning of the experiment and then fell into an unsaturated zone just after the end of the flushing-out period (week 13^{th}). The *SIs* variations of both minerals in HBD_5 and HBD_{10} revealed that Ca^{2+} concentration was controlled by the solubility of gypsum and those of calcite and dolomite. Moreover, over-saturated and saturated conditions of calcite and dolomite imply that those minerals did not increase leachate pH. In other words, when there was high enough MgO in the column (HBD_5 and HBD_{10}), MgO was hydrolyzed to $Mg(OH)_2$ and took control of the rising pH of the

effluents.

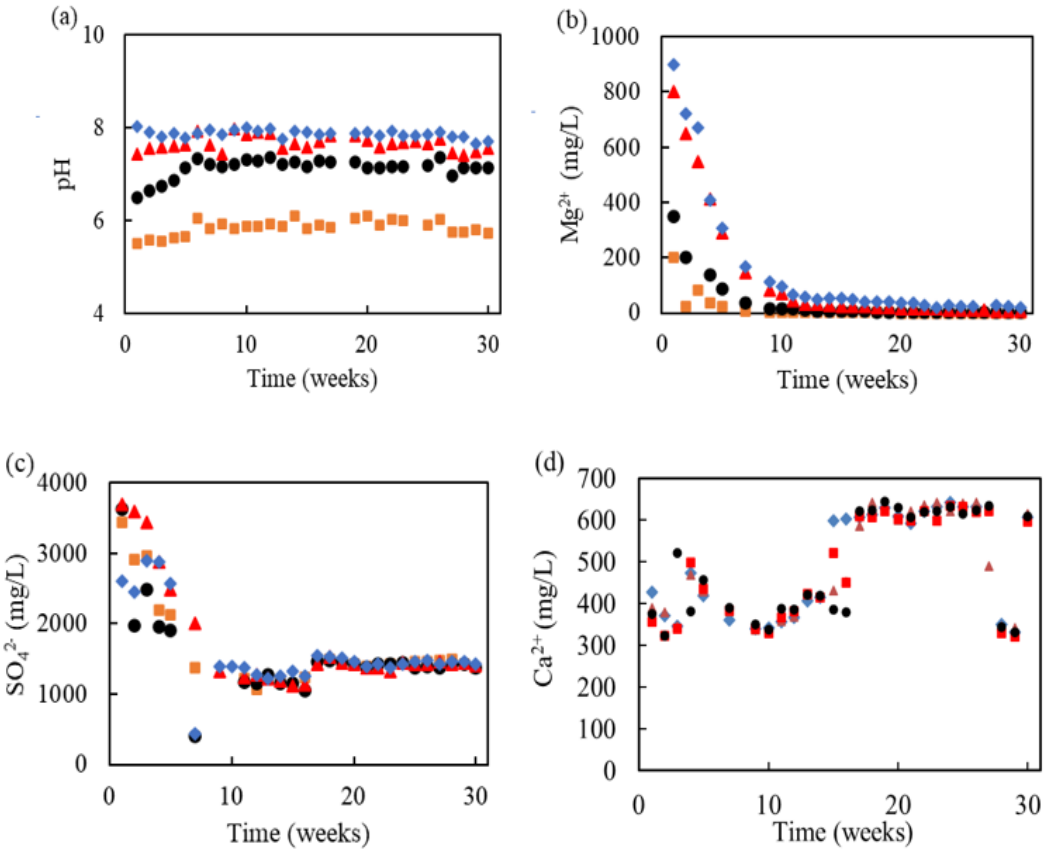

Figure 17. Changes in pH, Mg^{2+}, SO_4^{2-}, and Ca^{2+} concentrations over time: pH vs time (a), Mg^{2+}vs time (b), SO_4^{2-} concentration vs time (c), and Ca^{2+} concentration vs time (d) (case HBD_0 (■), case HBD_1 (●), case HBD_5 (▲), and case HBD_{10} (◆))

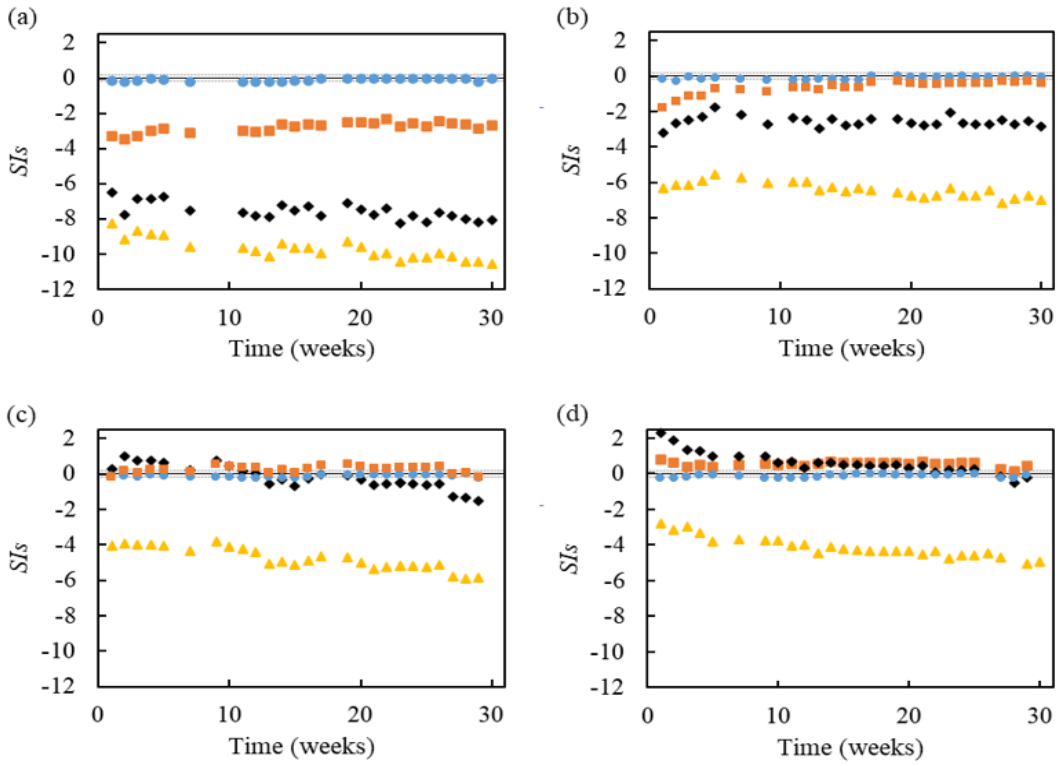

Figure 18. Saturation indices of Gypsum (●), Calcite (■), Dolomite (◆) and $Mg(OH)_2$ (▲) in the effluents of cases HBD_0 (a), HBD_1 (b), HBD_5 (c), and HBD_{10} (d)

4.3.3 Effects of HBD on heavy metals release

Figures 19(a-b) show the change of Pb and Zn concentrations in the effluent over time in all the columns. Lead and Zn were the toxic metals of concern since MRM (HBD_0) concentrations exceeded Zambia's effluent and wastewater values for Pb and Zn (The Zambia Environmental Management Act, 2013). The leaching concentration of Pb in case HBD_0 exhibited hill-shaped patterns during the first 11 weeks of the study before becoming relatively stable until the 30th week. The addition of HBD was more apparent to immobilize Pb since only HBD_1 could reduce the leaching concentration after the first week. However, HBD_5 was enough to suppress the leaching concentration of Pb lower than its regulatory limit (0.5 mg/L) at the beginning of the experiments. The leachability of Zn in cases HBD_0, HBD_1, and HBD_5 followed similar trends. It was initially high but rapidly decreased over time and stabilized after the 10th week in columns HBD_0, HBD_1,

and HBD_5, respectively. After the 10^{th} week, HBD_5 was enough to bring a long-term leaching concentration of Zn down below its regulatory value. However, the addition of HBD_{10} reduced Zn concentration in the effluent below the regulated value from the beginning toward the end of the experiment, and it only took three weeks to suppress the leaching concentration of Zn below the detection limit ICP-AES (0.1 mg/L). These results indicate that the HBD effectively immobilized Pb and Zn over a prolonged time.

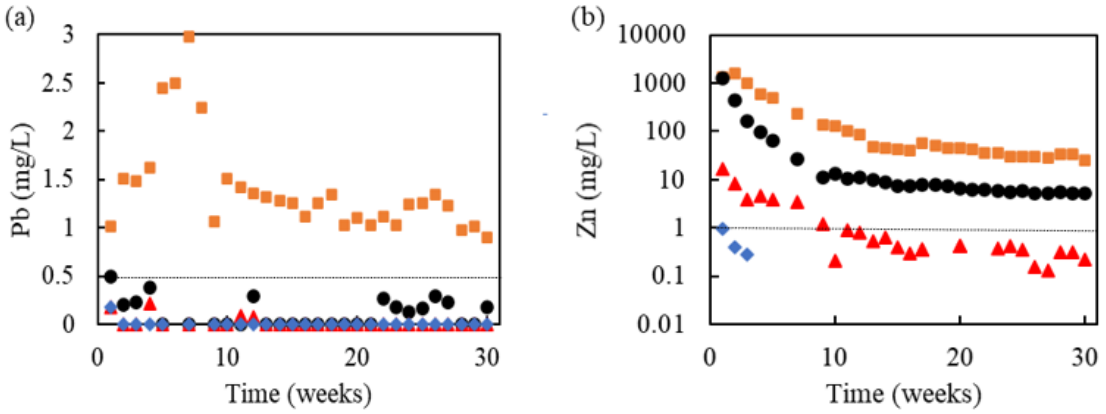

Figure 19. Changes in heavy metal concentrations over time: Pb (a) and Zn (b) (HBD_0 (■), HBD_1 (●), HBD_5 (▲), and HBD_{10} (◆)) (dash lines represent the effluent standard in Zambia)

4.3.4 Solid-phase partitioning and the liming effect of HBD

Figures 20a and b illustrate the change of Pb and Zn contents by sequential extraction of fresh MRM and residues of the columns. When the average precision of 7% is considered, the oxidizable and residual phase contents remain unchanged. The identical residual contents emphasize that they were significantly stable and did not leach and deposit. However, Pb and Zn are expected to be released from the oxidizable minerals (e.g., oxidation of pyrite, spherite, and galena). The assumption is due to the following reasons: sulfide minerals were expected to be available even though they could not be detected by XRD, and the experiments were done under atmospheric conditions in which oxygen in the atmosphere was freely dissolved and reacted with sulfide minerals. Based on the mass balance calculations, Pb and Zn were leached at the maximum amounts of ca. 0.02% and 3.5%, which are less than the average precision of the current employed sequential extraction technique (7%). According to the last reason, we should not have observed any metal content changes within the same fraction among all samples.

However, noticeable differences in Pb and Zn contents were detected within the exchangeable, carbonate, and reducible fractions. The changes in Pb and Zn fractionations among the three fractions played an essential role in controlling their mobility, allowing us to identify both metals' immobilization mechanisms by HBD.

The exchangeable contents of both metals were generally lower in the columns (HBD_1, HBD_5, and HBD_{10}) than those in fresh MRM, indicating that this fraction is an essential source of Pb and Zn. The exchangeable Pb decreased following the trend MRM > HBD_0 > HBD_1 > HBD_5 > HBD_{10}. The reduction of exchangeable Pb content with the amount of HBD addition most likely occurred due to the formation of carbonates, meaning the released Pb precipitated as carbonates, limiting the dissolution of soluble salts ($PbSO_4$) (Cappuyns et al., 2014). This interpretation is supported by a significant negative correlation between the exchangeable Pb content and the average pH value of the leachate from each column (r = 0.97 at the 0.05 significance level) (Figure 21). The content of exchangeable Zn was reduced to almost zero in cases HBD_0 and HBD_1 and zero in the other columns because of the dissolution of $ZnSO_4$ since it is easily soluble (Ferella et al., 2010). The carbonate contents of both metals in HBD_0 were lower than those in the fresh MRM. This clearly shows that, without treatment, Pb and Zn also leached from the carbonate fraction due to the acid dissolution of carbonate minerals supported by the leachate's moderate acidic pH in HBD_0 (Helser and Cappuyns, 2021).

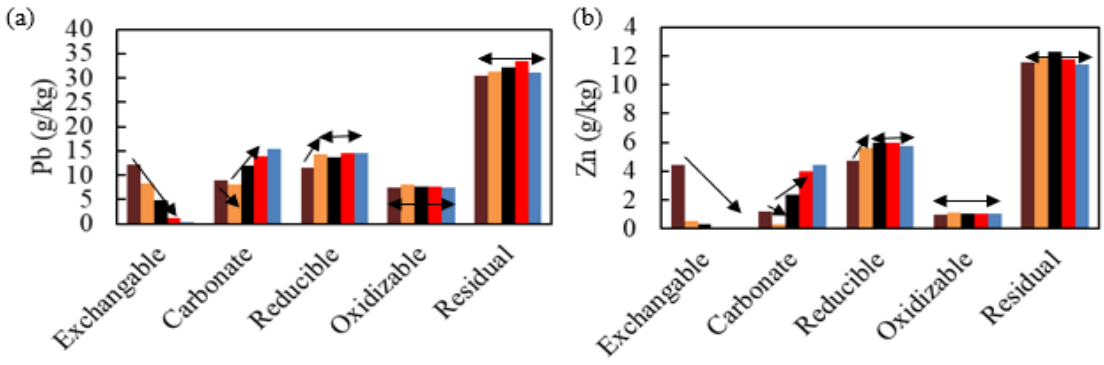

Figure 20. Changes in Pb (a) and Zn (b) contents of fresh MRM (■) and the residuals of HBD_0 (■), case HBD_1 (■), case HBD_5 (■), and case HBD_{10} (■)

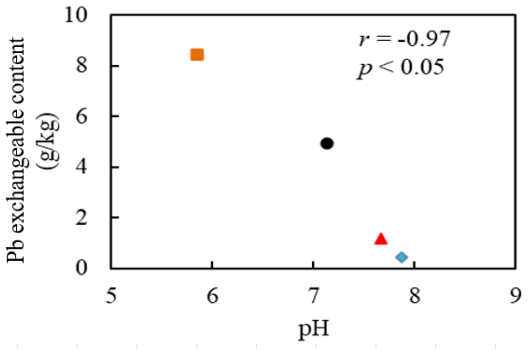

Figure 21. Exchangeable content of Pb in the residuals of cases HBD_0 (■), HBD_1 (●), HBD_5 (▲), and HBD_{10} (◆)

On the contrary, in the columns with HBD addition, the carbonate contents of Pb and Zn were higher than those of the fresh MRM and increased with the amount of HBD addition. These results reveal that the addition of HBD immobilized Pb and Zn as carbonate fractions due to HBD's abundance of calcite, dolomite, and magnesia. These minerals are known to have the ability to adsorb Pb and Zn (Gruszecka-Kosowska et al., 2017; Trakal et al., 2011). Since the precipitations of calcite and dolomite proved to be thermodynamically favorable (Figures 17c and d), co-precipitation of Pb and Zn with calcite and dolomite was also expected in HBD_5 and HBD_{10} (Ahmad et al., 2012, Godelitsas et al., 2007).

The reducible contents of Pb and Zn were higher in all residuals than those in the fresh MRM. Interestingly, regardless of the amount of HBD addition, the contents of both metals remained unchanged. The results imply the deposition of Pb and Zn in the reducible fraction over time, but HBD did not play a role in such an event. Theoretically, as pH increases, freer divalent Pb (Pb (II)) and Zn (Zn (II)) should be precipitated as hydroxides and/or be adsorbed or co-precipitated with iron-(oxy)hydroxides. There are two possible explanations for this phenomenon as follows:1) competition between the solubility of the hydroxides and the other immobilization mechanisms of Pb and Zn and 2) change in aqueous specifications of Pb (II) and Zn (II). As mentioned earlier, the pH alteration by HBD led to more immobilization of Pb and Zn as carbonate forms. Likewise, Pb (II) and Zn (II) in the leachate decreased, hindering their hydroxide precipitation potential. The reduction of Pb (II) and Zn (II) could also occur via the formation of carbonate and hydroxide complexes of Pb and Zn. These ions do not only hinder Pb- and

Zn-hydroxide precipitation potential but also inhibit the abilities of Pb and Zn to get absorbed and co-precipitated onto/with iron-(oxy) hydroxides since they tend to have a larger size with a lower charge compared to those of Pb (II) and Zn (II) (Badawy et al., 2000; Namie'snik and Rabajczyk, 2010; Powell et al., 2009).

However, the higher leachate pH by the liming effect of HBD could result in the precipitations of Pb-and Zn-carbonate minerals like cerussite, smithsonite, hydrocerussite, and hydrozincite. Figures 22a-d illustrate the *SIs* for the minerals mentioned above. Note that the *SIs* of the minerals of concern could not be obtained in the leachates having lower concentration(s) of Pb, Zn, or both than the detection limit of ICP-AES. In HBD_0, those carbonate minerals were unable to precipitate (*SI(s)* << -0.2) even though Pb and Zn leached at the highest concentrations. Conversely, in HBD_1, except for Pb-carbonates at the first four weeks of the experiment, at least one of the Pb- and Zn-carbonate minerals were saturated or supersaturated (*SI(s)* > -0.2) in most effluents over the experimental period. The low *SIs* values of the Pb-carbonates at the beginning of the experiment were probably due to the lower effluent pH. In cases HBD_5 and HBD_{10}, whenever the leaching concentration of Pb was over the detection limit of ICP-AES, *SIs* of Pb-carbonates were greater than -0.2. For Zn, the *SI* of only hydrozincite was thermodynamically favorable to precipitate first and then reduced to the unsaturated zone afterward. It should be noted that the unsaturated condition of hydrozincite was observed only when Zn concentration was very low (below the regulatory value of Zn). These results show that Pb- and Zn-carbonates could precipitate and control Pb and Zn mobility in the cases with HBD addition. However, Pb's mobility in the first few weeks of case HBD_1 tends to be dominantly controlled by the carbonate adsorption. In contrast, Zn's mobility at the low concentration zone could be governed by carbonate adsorption, co-precipitation with carbonate minerals, or both.

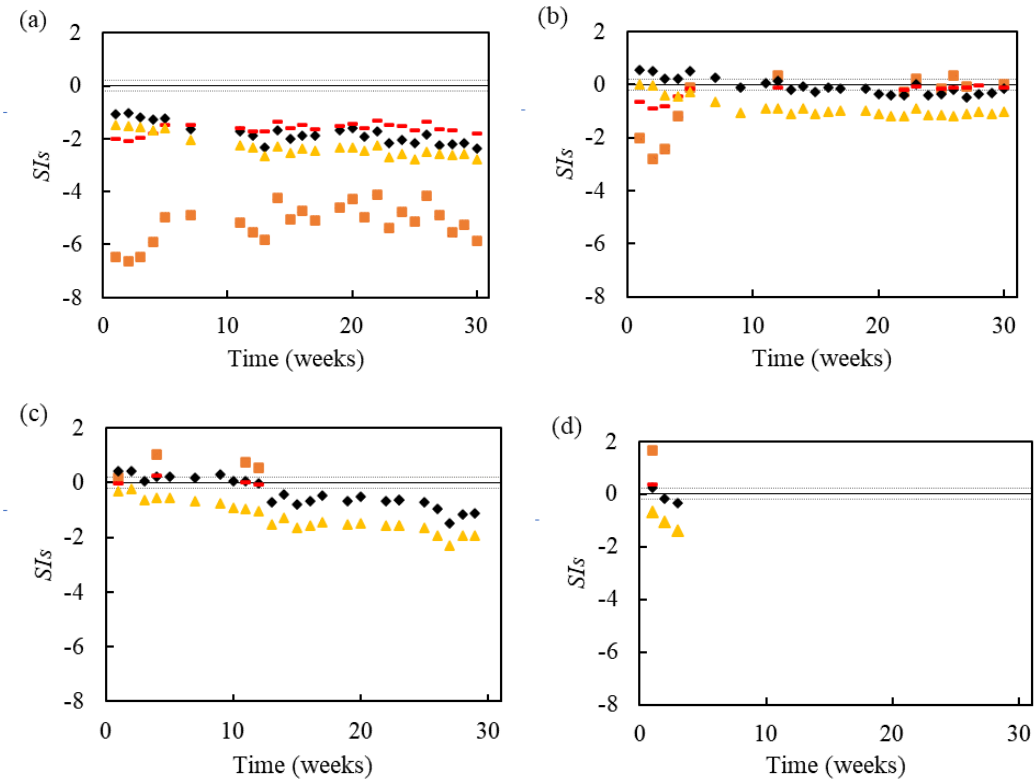

Figure 22. Saturation indices of cerussite (■), smithsonite (▲), hydrocerussite (■), and hydrozincite (◆) in the effluents of cases HBD_0 (a), HBD_1 (b), HBD_5 (c), and $HBDD_{10}$ (d)

4.3.5 Comparison with the leaching of Pb and Zn in pilot-scale experiments

Since 10% HBD could effectively immobilize the Pb and Zn in the first week of the experiments. Figure 23 and 24 shows the leaching results of MRM in the embankments with four case scenarios in pilot-scale experiments. With 10% HBD (Figure 23), the Pb and Zn were immobilized (cases 1 and 2). In cases 3 and 4 without 10% HBD to MRM, Zn leached out (Figure 24). The 10% HBD in cases 1 and 2 effectively immobilized the Pb and Zn by converting them into carbonate fractions. This is observed in the increase of pH in cases 1 and 2. However, in cases 3 and 4, the pH was precisely the same as fresh MRM. This could the reason why Zn leached out in those enbankments. The addition of 10% HBD with soil at the base of each embankment prevented the release of Pb and Zn at the bottom of each embankment. The results suggest that 10% HBD addition to MRM could effectively attenuate Pb and Zn in actual field conditions, thus preventing toxic elements from leaching into the groundwater.

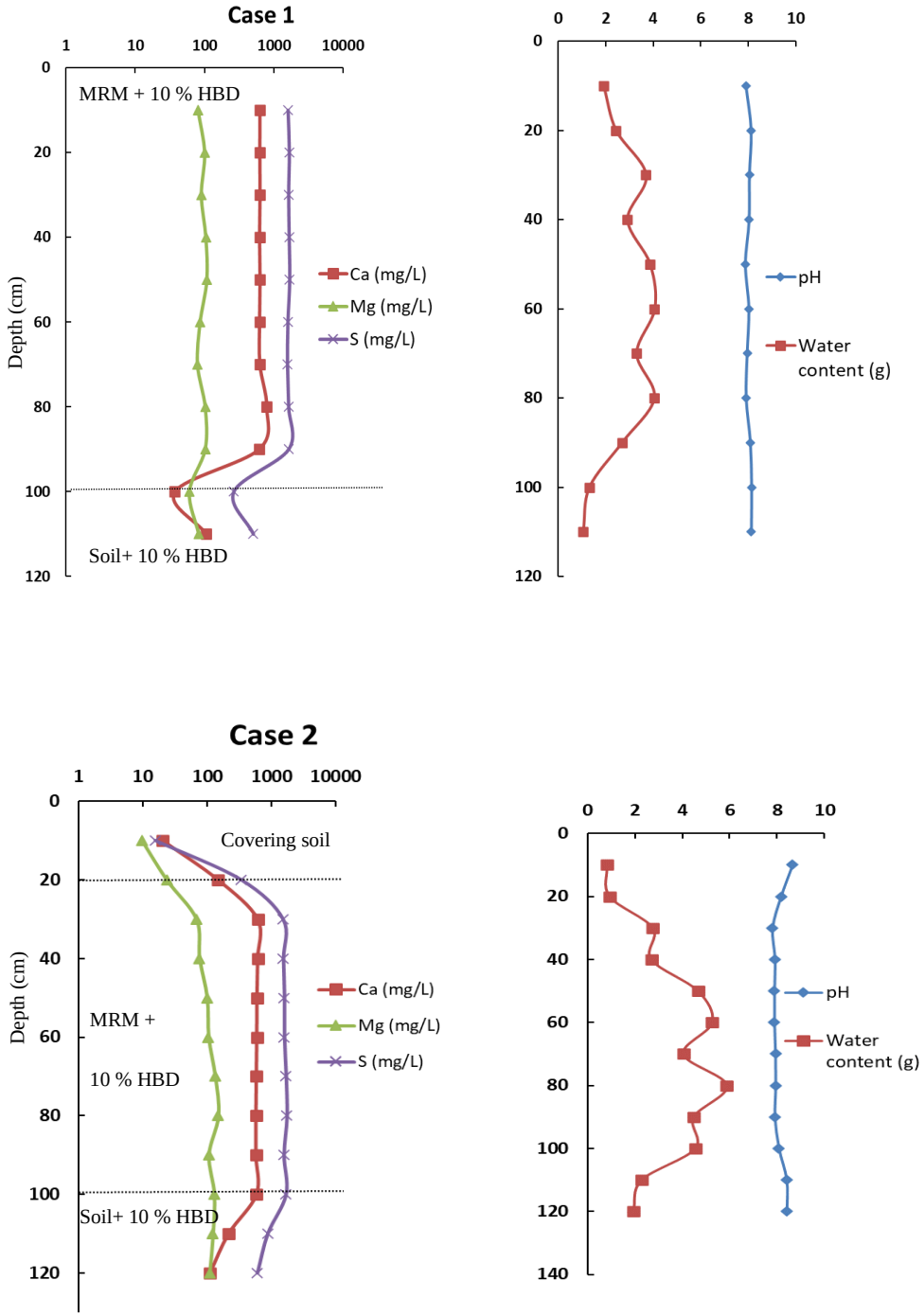

Figure 23. Leaching characteristics of mining residue material (MRM) and their related pH and water content in cases 1 and 2 with 10% HBD in the embankments.

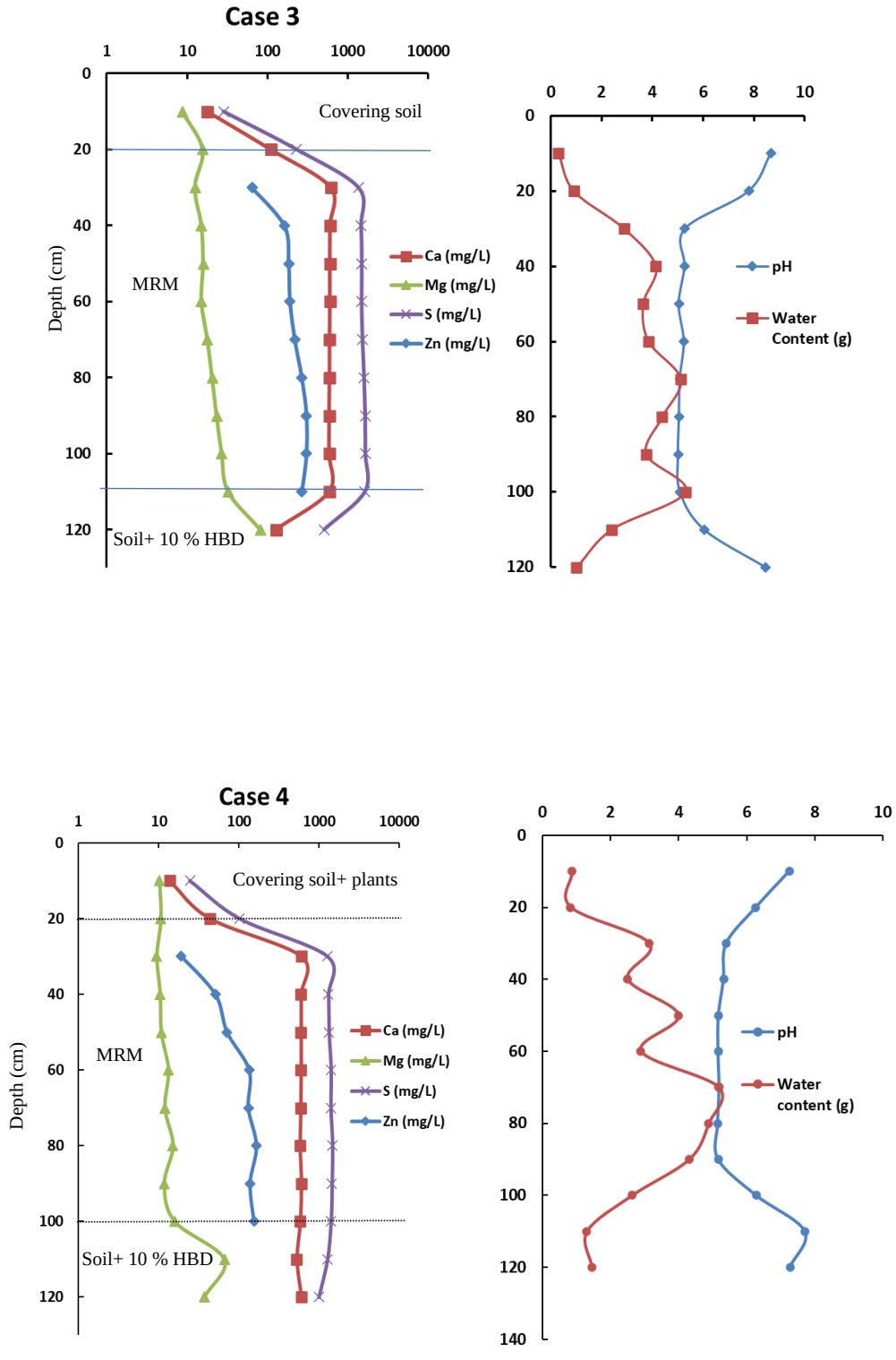

Figure 24. Leaching characteristics of mining residue material (MRM) and their related pH and water content in cases 3 and 4 without HBD of the embankments.

5. Conclusion

This chapter discussed the performance of HBD in immobilizing Pb and Zn leached from MRM using laboratory column experiments and the effectiveness of 10% HBD in actual field conditions i.e., pilot- scale experiments. The significant findings of the present study are summarized as follows:

The MRM was collected from Kabwe, Zambia, and the HBD was a heat-modified product of dolomite's naturally abundant material in Zambia. The column method was selected to mimic the actual implementation of the chemical immobilization technique. The HBD addition increased pH in both column and pilot experiments, thus lowering Pb and Zn migration. Ten percent HBD addition (HBD_{10}) was adequate to bring both Pb and Zn's leaching concentrations below the Zambian effluent standard and had a lasting effect on the system throughout the 30 weeks. Sequential extractions of pre-and post-experimental MRM revealed that Pb and Zn were mainly leached from exchangeable and carbonate phases, but portions of them were redeposited in reducible fractions. Adding HBD could not reduce the release of exchangeable Pb and Zn. However, it changed exchangeable Pb and Zn to carbonate and reducible ones, thereby reducing the potential sources of Pb and Zn. The carbonate contents of both Pb and Zn were higher than those of the pre-experimental MRM and increased with the amount of HBD added, suggesting that the addition of HBD permitted the columns to attenuate Pb and Zn as carbonate forms. The effectiveness of 10% HBD was validated in pilot-scale experiments and 10% HBD addition to the MRM in pilot-scale experiments prevented the leaching of Pb and Zn into the groundwater. Thus, the columns and pilot experiments verify the immobilization of MRM by 10% HBD.

References

Ahmad K., Bhatti, I.A., Muneer, M., Iqbal M, and Iqbal ,Z., 2012. Removal of heavy metals (Zn, Cr, Pb, Cd, Cu and Fe) in aqueous media by calcium carbonate as an adsorbent. Int J Chem Biol Sci 2, pp. 48-53.

Ali, A., Guo, D., Zhang, Y., Sun, X., Jiang, S., Guo, Z., Huang, H., Liang, W., Li, R. and Zhang, Z., 2017. Using bamboo biochar with compost for the stabilization and phytotoxicity reduction of heavy metals in mine-contaminated soils of China. Sci. Rep. 7(1), pp. 1-12.

Andrunik, M., Wołowiec, M., Wojnarski, D., Zelek-Pogudz, S. and Bajda, T., 2020. Transformation of Pb, Cd, and Zn minerals using phosphates. Minerals 10(4):342.

Anju, M., and Banerjee, D.K., 2010. Comparison of two sequential extraction procedures for heavy metal partitioning in mine tailings. Chemosphere 78(11), pp. 1393-1402.

Badawy, S.H., Helal M.I., Chaudri, A.M., Lawlor, K and McGrath, S.P., 2002. Soil solid-phase controls lead activity in soil solution. J. Environ. Qual. 31(1):pp. 162-167.

Banzhaf, S. and Hebig, KH., 2016. Use of column experiments to investigate the fate of organic micropollutants-A review. Hydrol. Earth. Syst Sci. 20(9), pp. 3719-3737.

Bolan, N., Kunhikrishnan, A., Thangarajan, R., Kumpiene, J., Park J., Makino T., Kirkham, M.B. and Scheckel, K., 2014. Remediation of heavy metal (loid)s contaminated soils-to mobilize or to immobilize? J. Hazard Mater. 266,pp. 141-166.

Cappuyns, V., Alian, V., Vassilieva, E. and Swennen, R., 2014. pH-dependent leaching behavior of Zn, Cd, Pb, Cu and As from mining wastes and slags: Kinetics and mineralogical control. Waste and Biomass Valorization 5(3), pp. 355-368.

Chandra, A.P and Gerson, A.R., 2010. The mechanisms of pyrite oxidation and leaching: A fundamental perspective. Surf. Sci. Rep. 65(9),pp. 293-315.

Clevenger, T.E., 1990. Use of sequential extraction to evaluate the heavy metals in mining wastes. Water Air Soil Pollut. 50(3), pp. 241-254.

Dang, Z., Liu, C. and Haigh, M.J., 2002. Mobility of heavy metals associated with the natural weathering of coal mine spoils. Environ. Pollut. 118(3),pp. 419-426.

Farrell M. and Jones D.L., 2010. Use of composts in the remediation of heavy metal contaminated soil. J. Hazard. Mater. 175(1-3), pp. 575-582.

Ferella F., De, Michelis I., Beolchini F., Innocenzi V. and Vegliò F., 2010. Extraction of zinc and manganese from alkaline and zinc-carbon spent batteries by citric-sulphuric acid solution. Int. J. Chem. Eng. 2010.

Fu J., He Q., Miedziak PJ., Brett GL., Huang X., Pattisson S., Douthwaite M. and Hutchings GJ., 2018. The role of $Mg(OH)_2$ in the so-called "base-free" oxidation of glycerol with AuPd catalysts. Chemistry - A European Journal 24(10), pp. 2396-2402.

Godelitsas, A., Kokkoris, M. and Misaelides, P., 2007. Investigation of the interaction of Greek dolomitic marble with metal aqueous solutions using Rutherford backscattering and X-ray photoelectron spectroscopy. J Radioanal and Nucl Chem 272(2), pp. 339-344.

Gray, C.W., Dunham, S.J., Dennis, P.G., Zhao, F.J. and McGrath S.P., 2006. Field evaluation of in situ remediation of a heavy metal contaminated soil using lime and red-mud. Environ. Pollut. 142(3), pp. 530-539.

Gruszecka-Kosowska, A., Baran, P., Wdowin, M. and Franus, W., 2017. Waste dolomite powder as an adsorbent of Cd, Pb (II), and Zn from aqueous solutions. Environ. Earth Sci. 6(15), pp. 1-12.

Hayes, S.M., White, S.A., Thompson, T.L., Maier, R.M. and Chorover, J., 2009. Changes in lead and zinc lability during weathering-induced acidification of desert mine tailings: Coupling chemical and micro-scale analyses. Appl. Geochem. 24(12),pp. 2234-2245.

He, M., Shi, H., Zhao, X., Yu, Y. and Qu, B., 2013. Immobilization of Pb and Cd in contaminated soil using nano-crystallite hydroxyapatite. Procedia Environ. Sci. 18, pp. 657-665.

Helser, J. and Cappuyns V., 2021. Trace elements leaching from pbzn mine waste (plombières, belgium) and environmental implications. J. Geochem. Explor. 220:106659.

Huyen, D.T., Tabelin, C.B., Thuan, H.M., Dang, D.H., Truong, PT., Vongphuthone, B., Kobayashi, M. and Igarashi, T., 2019. The solid-phase partitioning of arsenic in unconsolidated sediments of the Mekong Delta, Vietnam and its modes of release under various conditions. Chemosphere 233, pp. 512-523.

Khoeurn, K., Sasaki, A., Tomiyama, S. and Igarashi, T., 2018. Distribution of zinc, copper, and iron in the tailings dam of an abandoned mine in Shimokawa, Hokkaido, Japan. Mine Water Environ 38(1) pp. 119-129.

Kumpiene, J., Lagerkvist, A. and Maurice, C., 2008. Stabilization of As, Cr, Cu, Pb and Zn in soil using amendments- A review. J. Waste Manag. 28(1), pp. 215-225.

Lindsay, M.B., Moncur, M.C., Bain, J.G., Jambor, J.L., Ptacek, C.J. and Blowes, D.W., 2015. Geochemical and mineralogical aspects of sulfide mine tailings. Appl. Geochem. 57, pp. 157-177.

Liu, Z. and Dreybrod, W., 1997. Dissolution kinetics of calcium carbonate minerals in H_2O-CO_2 solutions in turbulent flow: The role of the diffusion boundary layer and the slow reaction $H_2O + CO_2 \leftrightarrow H^+ + HCO_3^-$. Geochem. Cosmochim. Acta. 61(14), pp. 2879-2889.

Liu, L., Li, W., Song, W., Guo M., 2018. Remediation techniques for heavy metal-contaminated soils: Principles and applicability. Sci. Total. Environ. 633,pp. 206-219.

Mahar, A., Ping, W.A., Ronghua, L.I. and Zhang, Z., 2015. Immobilization of lead and cadmium in contaminated soil using amendments: A review. Pedosphere 25(4), pp. 555-568.

Marumo, K., Ebashi, T. and Ujiie,T., 2003. Heavy metal concentrations, leachabilities, and lead isotope ratios of Japanese soils. Shigen Chihsitsu 53, pp. 125-146 (In Japanese).

Namie'snik, J. and Rabajczyk, A., 2010. The speciation and physicochemical forms of metals in surface waters and sediments. Chem. Speciat. Bioavailab. 22(1), pp 1-24.

Nordstrom, D.K. and Alpers, C.N., 1999. Negative pH, efflorescent mineralogy, and consequences for environmental restoration at the iron mountain superfund site, California. Proc. Natl. Acad. Sci. 96(7), pp. 3455-3462.

Parkhurst, D.L. and Appelo, C.A., 1999. User's guide to PHREEQC (Version 2): A computer program for speciation, batch-reaction, one-dimensional transport, and inverse geochemical calculations. Water Resources Investigation Report. 99(4259):312.

Pehlivan, E., Özkan, A.M., Dinç, S. and Parlayici, Ş., 2009. Adsorption of Cu^{2+} and Pb^{2+} ion on dolomite powder. J. Hazard. Mater. 167(1-3), pp. 1044-1049.

Pokrovsky, O.S. and Schott, J.N., 200. Kinetics and mechanism of dolomite dissolution in neutral to alkaline solutions revisited. Am. J. Sci. 301, pp. 597-626.

Powell KJ., Brown PL., Byrne RH., Gajda T., Hefter G., Leuz AK., Sjöberg S. and Wanner H., 2009. Chemical speciation of environmentally significant metals with inorganic ligands, Part 3. The Pb^{2+}, OH^-, Cl^-, CO_3^{2-}, SO_4^{2-}, and PO_4^{3-} systems. IUPAC Technical Report. Pure Appl. Chem. 81, pp. 2425-2476.

Seshadri, B., Bolan, N.S., Choppala, G., Kunhikrishnan, A., Sanderson, P., Wang, H., Currie, L.D., Tsang, D.C., Ok, Y.S. and Kim, G., 2017. Potential value of phosphate compounds in enhancing immobilization and reducing bioavailability of mixed heavy metal contaminants in shooting range soil. Chemosphere 184, pp. 197-206.

Tabelin, C.B., Igarashi, T and Tamoto, S., 2010. Factors affecting arsenic mobility from hydrothermally altered rock in impoundment-type in situ experiments. Miner. Eng. 23(3), pp. 238-248.

Tabelin, C.B., Igarashi, T. and Yoneda, T., 2012. Mobilization and speciation of arsenic from hydrothermally altered rock containing calcite and pyrite under anoxic conditions. Applied geochemistry, 27(12), pp. 2300-2314.

Tabelin, C.B., Igarashi, T., Arima, T., Sato, D., Tatsuhara, T. and Tamoto, S., 2014. Characterization and evaluation of arsenic and boron adsorption onto natural geologic materials, and their application in the disposal of excavated altered rock. Geoderma 213, pp. 163-172.

Tangviroon, P., Hayashi, R and Igarashi, T., 2017. Effects of additional layer(s) on the mobility of arsenic from hydrothermally altered rock in laboratory column experiments. Water Air Soil Pollut. 228(5), pp. 1-10.

Tangviroon, P. and Igarashi T., 2017. Modeling and evaluating the performance of river sediment on immobilizing arsenic from hydrothermally altered rock in laboratory column experiments with Hydrus-1D. Water Air Soil Pollut., 228(12), pp. 1-12.

Tessier A., Campbell G.C. and Bisson M., 1979. Sequential extraction procedure for the speciation of particulate trace metals. Anal. Chem. 51(7),pp. 844-851.

The Environment Management Act. The environment management (licensing) regulations. SI Govt. Zambia 2013. 112, pp. 737-858.

Trakal, L., Neuberg M., Tlustoš P., Száková J., Tejnecký V. and Drábek O., 2011. Dolomite limestone application as a chemical immobilization of metal-contaminated soil. Plant Soil Environ 57(4), pp. 173-179.

Valente T.M., Grande, J.A. and De la Torre, M.L., 2016. Magnesium and aluminum sulfates in salt efflorescences from acid mine drainage in the Iberian Pyrite Belt (SW Spain). Proceedings IMWA Freiberg/Germany,pp. 445-450

Vongphuthone, B., Kobayashi, M and Igarashi T., 2017. Factors affecting arsenic content of unconsolidated sediments and its mobilization in the Ishikari Plain, Hokkaido, Japan. Environ. Earth Sci. 76(19), pp. 1-11.

Vrînceanu, N.O., Motelică, D.M., Dumitru, M., Calciu, I., Tănase, V. and Preda, M., 2019. Assessment of using bentonite, dolomite, natural zeolite and manure for the immobilization of heavy metals in a contaminated soil: the Copșa Mică case study (Romania). Catena 176,pp. 336-342.

Xing, Z., Bai, L., Ma, Y., Wang, D. and Li, M., 2018. Mechanism of magnesium oxide hydration based on the multi-rate model. Materials 11(10):1835.

Chapter 5

GENERAL CONCLUSION

Kabwe Town in Zambia is characterized by massive mine wastes containing toxic elements like Pb and Zn. These mine wastes are responsible for the contamination of soils in the city; consequently, high blood Pb levels in the children of Kabwe result from the legacy mining. Therefore, the present study was conducted to evaluate the extent of pollution and bioaccessibility of Pb and Zn in one of the potential sites for Pb intoxication in children, i.e., school playground soils. To curb the contamination of soils in Kabwe, we also evaluated the effectiveness of half-burnt dolomite in immobilizing Pb and Zn from the mining residual materials (MRM). Laboratory experiments such as batch leaching tests, sequential extraction, XRD-XRF, SEM-EDS, and TC/IC analyses, were performed to achieve this goal. The general conclusions were divided into four parts, which corresponded to four chapters of this dissertation

Chapter 1 briefly introduced Pb contamination in Kabwe and provided an overview of Pb intoxication and some of the remediation proposals that have been conducted in Kabwe.

Chapter 2 was conducted to find the leachability, solid-phase partitioning, and extent of contamination in Kabwe school playground soils near the mine area. The anthropogenic contamination and enrichment of Pb and Zn in the playground were traced back to the old mining activities. The playground soils had high enrichment of Pb and Zn. The Pb and Zn in the soils were mainly bound with the carbonates, reducible and oxidizable phases. The labile phases' bioaccessible fractions of Pb and Zn were exceptionally high for all the playground soils. The results suggest that the playground soils are potential sources of toxic elements for the children in Kabwe. Therefore, the human health risk associated with inhalation/ingestion of toxic elements from the soils is high. Revegetation, soil turning, and watering of the playgrounds to suppress dust generation could be short-term measures to reduce the high bioaccessibility of Pb and Zn in the playgrounds.

After identifying that the playgrounds are a potential source of Pb and Zn intoxication for the children, Chapter 3 then assessed the primary exposure routes for the

uptake of Pb into the bloodstream of the children in Kabwe. The efficacy of simulated fluids (artificial lysosomal fluid (ALF), gamble solution (GS), and phosphate-buffered (PBS) and HC*l* in the dissolution of Pb and Zn from mining residual materials and soil samples were assessed. The higher solubility of Pb and Zn was observed with HC*l* extraction compared to the simulated fluids. The HC*l* aggressively dissolves the exchangeable, carbonates and Fe/Mn oxides. Comparing exposure routes, i.e., inhalation and ingestion for the uptake of Pb from contaminated soil or mine wastes, ingestion is more apparent. The high Pb blood levels found in the residents of Kabwe can be related to ingestion of contaminated soil or dust containing high levels of Pb. Substantial amounts of Pb could be released in the stomach (low pH), resulting in high adsorption of the toxic element into the bloodstream. Children are likely to be more affected than adults because of their hand-to-mouth activities. In addition, the solid-phase partitioning of the mining residual materials showed that, regardless of particle size, the contents of Pb and Zn did not significantly change. However, at least 33% of Pb in the (exchangeables, carbonates, and Fe/Mn oxides were mobilizable under acidic conditions. These results implied that substantial amounts of Pb could be available for adsorption in case of accidental ingestion of the residual materials.

To reduce the high bioaccessibility of Pb and Zn, Chapter 4 assessed the long-term potency of half-burnt dolomite (HBD) in immobilizing Pb and Zn leached from mining residual materials. The HBD addition increased pH in both column and pilot experiments, thus lowering Pb and Zn migration. Ten percent addition of HBD (HBD_{10}) was adequate to bring both Pb and Zn's leaching concentrations below the Zambian effluent standard and had a lasting effect on the system throughout the 30 weeks. Sequential extractions of pre-and post-experimental MRM revealed that Pb and Zn were mainly leached from exchangeable and carbonate phases, but portions of them were redeposited in reducible fractions. The primary attenuation mechanism in both column and pilot experiments was the precipitation of Pb and Zn into carbonate complexes.

Thus, the columns and pilot experiments verify immobilization of MRM by 10% HBD. The attenuation of Pb and Zn could occur via adsorption, co-precipitation, and precipitation mechanisms. Kabwe pollution problem and the high bioaccessible fractions of Pb and Zn could significantly be reduced by the application of 10% HBD to the MRM. The HBD has shown to be an effective immobilizer that can be used in actual field

conditions in Zambia. The cheap immobilizer can be utilized on a large scale in Zambia and this could greatly benefit the residents of Kabwe.

ACKNOWLEDGMENT

I would like to express my sincere gratitude to Prof. Toshifumi IGARASHI for giving me the opportunity to pursue the doctorate degree under his laboratory. His vast knowledge and wisdom, expert advice and support is out of this world. I'm so grateful to be one of the many students that he has trained across the world. His encouragement and guidance from the begining of my doctorate degree, enabled me to develop a deep understanding of my research.

I would like to also thank the evaluation committee members Prof Naoki HIROYOSHI, Associate Prof. Yasumasa TOJO and Prof. Tsutomu SATO for their guidance. I would like to express my sincere gratitude to Associate Prof. Shusaku HARADA and Assistant Prof. Takahiko ARIMA for their guidance in the laboratory.

I wish to thank all the KAMPAI members for their great support in Zambia and Japan, I wish to extend my sincere gratitude to Prof. Mayumi ITO, Prof. Mayumi ISHIZUKA, Associate Prof. Shouta NAKAYAMA, Prof. Imasiku NYAMBE, Dr. Hokuto NAKATA and Dr. Pawit TANGVIROON for their immerse support.

I would also like to thank all the laboratory members in the division for their help in experiments and fruitful discussions.

I would like to acknowledge The Japanese Government through The Ministry of Education, Culture, Sports, Science and Technology (MEXT) for giving me the scholarship to study in Japan

Finally, I would like to thank my Dad and Mom for their support throughout my life, you raised a good son!